Center-symmetric Landau gauge meets the lattice

Duifje Maria van Egmond,[1] Orlando Oliveira,[2] Urko Reinosa,[3] Julien Serreau,[4] Paulo J. Silva,[2] and Matthieu Tissier[5]

[1]*ICTP South American Institute for Fundamental Research Instituto de Física Teórica, UNESP—Universidade Estadual Paulista Rua Dr. Bento Teobaldo Ferraz 271, 01140-070, São Paulo, SP, Brazil*

[2]*CFisUC, Department of Physics, University of Coimbra, P-3004 516 Coimbra, Portugal*

[3]*Centre de Physique Théorique, CNRS, Ecole polytechnique, IP Paris, F-91128 Palaiseau, France*

[4]*Université Paris Cité, CNRS, Astroparticule et Cosmologie, F-75013 Paris, France*

[5]*Sorbonne Université, CNRS, Laboratoire de Physique Théorique de la Matière Condensée, 75005 Paris, France*

(Received 20 December 2024; accepted 20 May 2025; published 18 July 2025)

A lattice implementation of the recently introduced center-symmetric Landau gauge is discussed and its predictions confronted with numerical Monte Carlo simulations. It is shown that the link average and the link correlators computed in that gauge are order parameters of the confinement-deconfinement transition at nonzero temperature. Strictly speaking, this requires a specific treatment of the Gribov copies that we discuss in detail. The numerical simulations comply with the theoretical predictions for the link average computed below and above the deconfinement temperature. Our results show that, within appropriately chosen gauges, one can construct local order parameters for center symmetry, as proxies for the nonlocal Polyakov loop.

DOI: 10.1103/jcmj-jng4

I. INTRODUCTION

Center symmetry plays a pivotal role in the context of non-Abelian gauge theories and in particular quantum chromodynamics (QCD). Although not a symmetry of the QCD action, it becomes a strict symmetry in the limit of infinitely heavy quarks [1,2], just as chiral symmetry becomes a strict symmetry in the limit of massless quarks. And just as chiral symmetry is broken spontaneously at low temperatures, providing a mechanism of mass generation for the confined hadronic bound states, center symmetry can be broken at high temperatures, leading to a quark-gluon plasma phase [3–6]. It is then no doubt that these two symmetries play such a prominent role in the investigation of the phase structure of strongly interacting nuclear matter.

Describing the Yang-Mills (YM) confinement/deconfinement transition in the continuum is not straightforward, however. One issue comes from the necessary gauge fixing that can break the underlying center symmetry explicitly at the level of the gauge-fixed action [7]. Although this breaking should not be visible at the level of gauge-invariant order parameters such as the Polyakov loop [8], the latter are generically nonlocal observables, which are not of easy access in continuum calculations [9]. Moreover, gauge-invariant quantities can also be contaminated by the gauge-fixing symmetry breaking due to the necessary approximations or modeling employed in such approaches. Of course, this is a spurious effect which should diminish as one improves the degree of approximation, but it can have harmful consequences at the lowest orders of approximation.

For these various reasons, in the continuum, it is interesting to use gauge fixings that do not break the center symmetry explicitly, while offering the possibility to define alternative (and local) order parameters which are simpler to evaluate in practice. A major step in this direction was achieved in Refs. [10,11] where it was shown that the gauge-field average plays the role of an order parameter for center symmetry in the self-consistent background Landau gauge [12,13]. This approach, which has been quite successful in recent years [14], is not void of subtleties, however. In particular, the gauge-field average is obtained from the minimization of a functional which is not exactly a thermodynamical potential in the sense of a Legendre transform of the free-energy. One consequence is that the very identification of the gauge-field average with the minimum of this potential relies on additional assumptions which are not necessarily fulfilled in the presence of approximations or modeling [15].

Recently, an alternative proposal has been put forward in [7,16] where, rather than working with a self-consistent background, one uses a fixed center-symmetric background configuration in both the confined and deconfined phases. It was shown that in this so-called center-symmetric Landau gauge, the gauge field average, and more generally, the

Published by the American Physical Society under the terms of the Creative Commons Attribution 4.0 International license. Further distribution of this work must maintain attribution to the author(s) and the published article's title, journal citation, and DOI. Funded by SCOAP³.

gauge-field correlators are, in fact, local order parameters for center symmetry [17]. The main advantage here is that the functional to be extremized is a genuine Legendre transform, which thus eliminates the above-mentioned subtleties of the self-consistent background field approach.

Various tests of these theoretical expectations have been performed, showing that, in the center-symmetric Landau gauge, the one-point function [16] but also the two-point correlators [18] capture properly the nature of the transition as a function of the gauge group and give very good results for the deconfinement transition. So far, these tests have been conducted within the context of the Curci-Ferrari model [19], a simple extension of the Faddeev-Popov (FP) gauge-fixed Lagrangian which successfully captures many infrared aspects of YM theories (see Ref. [20] for a recent review).

Although the Curci-Ferrari model was pivotal in some of the above developments as it provided a framework where many quantities could be computed semianalytically, a serious test of the relevance of the center-symmetric Landau gauge should lift any source of modeling. In this work, we then propose a lattice implementation of the center-symmetric gauge fixing. We shall here restrict to the SU(3) case but the discussion can easily be extended to SU(N) along the lines of Ref. [17].

In Sec. II, we gather some generalities regarding the lattice setup, including the notions of links and plaquettes, the Wilson action, and the way observables are computed using Monte Carlo importance sampling. Section III discusses center symmetry and its breaking from the point of view of the gauge-invariant Polyakov loop. We put special emphasis on the very different nature of the Monte Carlo ensemble in the broken and unbroken phases. We also discuss charge conjugation as it plays a role in the following. In Sec. IV, we repeat the same discussion from the point of view of link correlators, which, in a sense, replace the gauge-field correlators of the continuum approach. As the correlators are gauge-dependent quantities, defined only once a gauge is fixed, we spend some time recalling the lattice gauge fixing procedure, paying particular attention to the issue of Gribov copies. We investigate the general conditions under which the link correlators actually become order parameters for center symmetry. This defines the class of center-symmetric gauges. Section V considers an explicit example of a center-symmetric gauge, closely related to the continuum one proposed in Ref. [16]. We identify and solve the symmetry constraints for the link average in that gauge and study whether and when these constraints are fulfilled within actual numerical simulations. Finally, Sec. VI gathers additional material such as an equivalent analysis in terms of twisted link variables, some remarks concerning the relation between the links and the gauge field, or the invariance properties of the gauge-fixed ensemble.

As a final word, let us mention that there exist various lattice studies that aim at tracking down the transition using gauge-field correlators in non-center-symmetric gauges, such as the standard Landau gauge [21–26], alongside similar studies in the continuum [27,28]. Although manifest changes of behavior have been reported for these quantities in the vicinity of the transition, some of which seem to mimic those of an actual order parameter, no rigorous connection exists to date between those observed behaviors and center-symmetry breaking. It is the purpose of the present work, together with Refs. [16,17], to provide a setup where such a connection can be clearly established.

One important exception is the study of Ref. [29] where a connection between center-symmetry breaking and differences of Landau gauge propagators over different ensembles of configurations (corresponding to different center sectors) was established. We stress that these results are not in contradiction with the discussion in the present work, but rather complementary. A detailed account of the two approaches will be discussed in a forthcoming work dedicated to the propagators.

II. GENERALITIES

We consider the lattice discretization of SU(3) Yang-Mills theory using link and plaquette variables. The sites of the lattice are described by a 4-vector n with integer components $n_\mu \in \mathbb{N}$, with $\mu = 1, 2, 3, 4$, $0 \leq n_\mu \leq L_\mu - 1$, where L_μ is the lattice extent along direction μ.

A. Links and plaquettes

We denote by $\hat{\mu}$ the vector of components

$$\hat{\mu}_\nu \equiv \delta_{\mu\nu}, \tag{1}$$

which connects a given site n to its neighboring site $n + \hat{\mu}$ along direction μ. With such an oriented link, one associates a link variable $U_\mu(n) \in \mathrm{SU}(3)$. Correspondingly, the oriented link connecting $n + \hat{\mu}$ to n is associated with the link variable $U_\mu^\dagger(n)$ also written as $U_{-\mu}(n + \hat{\mu})$. The thermal field theory setup considered in this work assumes periodic boundary conditions in all directions. The link variables can thus be extended over an infinite lattice such that

$$U_\mu(n + L_\nu \hat{\nu}) = U_\mu(n), \tag{2}$$

for any direction ν.

With the links at our disposal, we can consider more general constructs. In particular, an oriented plaquette is a square loop made of oriented links, starting at n and going through $n + \hat{\mu}$, $n + \hat{\mu} + \hat{\nu}$, $n + \hat{\nu}$, and back to n. With each such oriented loop, one associates the plaquette variable

$$U_{\mu\nu}(n) \equiv U_\mu(n)U_\nu(n+\hat{\mu})U_{-\mu}(n+\hat{\mu}+\hat{\nu})U_{-\nu}(n+\hat{\nu}) = U_\mu(n)U_\nu(n+\hat{\mu})U_\mu^\dagger(n+\hat{\nu})U_\nu^\dagger(n), \quad (3)$$

which is also an element of SU(3).

B. Wilson action and gauge invariance

The plaquette variables enter the definition of the Wilson action

$$S_W[U] \equiv \beta \sum_n \sum_{\mu<\nu} \mathrm{Re\,tr}[\mathbb{1} - U_{\mu\nu}(n)], \quad (4)$$

where $\beta = 2N/g^2$ and g denotes the bare coupling constant. The Wilson action is a discretized version of the gauge-invariant Yang-Mills action. Let us briefly recall how gauge invariance comes about.

A gauge transformation is defined by the choice, at each site n of the lattice, of an element $g_0(n) \in \mathrm{SU}(3)$ such that

$$g_0(n + L_\nu \hat{\nu}) = g_0(n), \quad (5)$$

for any direction ν (periodicity in all directions). Gauge transformations form a group denoted $\mathcal{G}_0$ in what follows. This includes global color rotations. Under a gauge transformation

$$U_\mu(n) \to g_0(n)U_\mu(n)g_0^\dagger(n+\hat{\mu}) \equiv U_\mu^{g_0}(n), \quad (6)$$

the plaquette variables transform as

$$U_{\mu\nu}(n) \to g_0(n)U_{\mu\nu}(n)g_0^\dagger(n), \quad (7)$$

and the Wilson action (4) is invariant.

C. Observables and Monte Carlo ensemble

Observables are obtained as expectation values of gauge-invariant functionals

$$\mathcal{O}[U^{g_0}] = \mathcal{O}[U], \quad (8)$$

weighted by the gauge-invariant probability distribution $\exp\{-S_W[U]\}$:

$$\langle \mathcal{O} \rangle \equiv \frac{\int \prod_{n,\mu} dU_\mu(n) \mathcal{O}[U] e^{-S_W[U]}}{\int \prod_{n,\mu} dU_\mu(n) e^{-S_W[U]}}. \quad (9)$$

In practice, this large multidimensional integral is evaluated using importance sampling Monte Carlo techniques. One first generates a finite ensemble

$$\mathcal{E} = \{U_\mu(n)\} \quad (10)$$

of link configurations that follow the probability distribution $\exp\{-S_W[U]\}$. Then, the observable is evaluated as

$$\langle \mathcal{O} \rangle \simeq \frac{1}{N_{\mathrm{conf}}} \sum_{U_\mu \in \mathcal{E}} \mathcal{O}[U] \equiv \langle \mathcal{O} \rangle_{\mathcal{E}}. \quad (11)$$

We shall refer to $\mathcal{E}$ as a Monte Carlo ensemble.

We note that the gauge invariance of $S_W[U]$ reflects the redundancy of the description of the system in terms of gauge fields and the Monte Carlo ensemble generated from $S_W[U]$ should reflect this redundancy. That is, for a sufficiently large ensemble, for any link configuration $U_\mu(n)$ in the ensemble, its $\mathcal{G}_0$-orbit, defined as $\{U_\mu^{g_0} | g_0 \in \mathcal{G}_0\}$, is faithfully represented in the ensemble. Of course, in practice, the gauge ensembles are finite, not necessarily large, but should provide good representations of the gauge manifold.

III. CENTER SYMMETRY

The gauge transformations in $\mathcal{G}_0$ leave the Wilson action invariant while preserving the periodicity of the link variables. As we now recall, however, these are not the only transformations endowed with these properties.

A. Center transformations

In particular, one can consider transformations

$$U_\mu(n) \to g(n)U_\mu(n)g^\dagger(n+\hat{\mu}) \equiv U_\mu^g(n) \quad (12)$$

that are periodic in the time direction but only modulo an element of the center of SU(3),[1]

$$g(n + L_4\hat{4}) = e^{i2\pi/3} g(n). \quad (13)$$

These are known as center transformations. Of course, $g^\dagger$ is also a center transformation with associated center element $e^{-i2\pi/3}$. Together with the periodic gauge transformations, they form a group denoted $\mathcal{G}$ in what follows, which contains $\mathcal{G}_0$ as a subgroup. From now on, we will exclusively use g_0 to denote periodic gauge transformations, i.e., transformations that belong to $\mathcal{G}_0$, while g or $g^\dagger$ will denote center transformations with a nontrivial center element.

That center transformations are symmetries of the Wilson action is obvious from the discussion in the previous section. However, even though they take the same form as gauge transformations, they do not qualify as genuine gauge transformations (in the sense of redundancies in the description of the system at hand) but, rather, as

[1]We could also consider center transformations along the other Euclidean directions. However, in the present finite temperature context, one should eventually consider the limit $L_\nu \to \infty$ with a fixed inverse temperature $L_4 a = 1/T$ and $L_i a \to \infty$, where a denotes the lattice spacing. In this case, only the temporal center transformations are relevant. We also stress that center transformations should not be mistaken with global color rotations equal to an element of the center of the group. The latter are periodic and, actually, do not change the links.

physical transformations. This is because they act nontrivially on some observables, an example of which is the Polyakov loop.

B. The Polyakov loop

The Polyakov loop is defined as the trace of a product of links that loop around the temporal direction:

$$\Phi[U](\vec{n}) \equiv \frac{1}{3}\mathrm{tr}U_4(n_0)U_4(n_0+\hat{4})U_4(n_0+2\hat{4})\cdots \\ \cdots U_4(n_0+(L_4-1)\hat{4}), \tag{14}$$

with $n_0 \equiv (\vec{n},0)$.[2]

Under a periodic gauge transformation g_0, one has

$$\Phi[U^{g_0}](\vec{n}) = \Phi[U](\vec{n}). \tag{15}$$

The Polyakov loop is then gauge-invariant, and its expectation value defines an observable

$$\langle\Phi\rangle \equiv \frac{\int\prod_{n,\mu}dU_\mu(n)\Phi[U](\vec{n})e^{-S_W[U]}}{\int\prod_{n,\mu}dU_\mu(n)e^{-S_W[U]}}, \tag{16}$$

referred to in what follows as the averaged Polyakov loop. Due to the translation invariance of the Wilson action and the use of periodic boundary conditions, this average does not depend on $\vec{n}$. As is well known, its physical interpretation is that, in the infinite volume and continuum limits, it corresponds to $e^{-\Delta F/T}$ where ΔF is the free-energy increase of a thermal bath of gluons at temperature T upon inclusion of a static color charge. It follows that the averaged Polyakov loop can be used to probe the confinement/deconfinement transition: a vanishing averaged Polyakov loop signals a confined phase ($\Delta F = \infty$), whereas a nonzero value signals a deconfined phase ($\Delta F < \infty$).

That $\langle\Phi\rangle$ can behave so differently depending on the temperature relies on the fact that the symmetry (12) can either be explicitly realized or spontaneously broken. One rigorous way to discuss this is to introduce a small perturbation to the Wilson action in the form of a source term[3] $\Delta S_W^{\rho,\theta}[U] \equiv \rho e^{i\theta}\sum_{\vec{n}}\Phi[U](\vec{n})$ which breaks the symmetry explicitly, and to study the fate of the Polyakov loop average

$$\langle\Phi\rangle_{\rho,\theta} \equiv \frac{\int\prod_{n,\mu}dU_\mu(n)\Phi[U](\vec{n})e^{-S_W[U]-\Delta S_W^{\rho,\theta}[U]}}{\int\prod_{n,\mu}dU_\mu(n)e^{-S_W[U]-\Delta S_W^{\rho,\theta}[U]}}, \tag{17}$$

in the limit $\rho \to 0^+$.

[2]We recall that $\hat{4} = (\vec{0},1)$ so that $n_0 + p\hat{4} = (\vec{n},p)$.

[3]The source $\rho e^{i\theta}$ coupled to the Polyakov loop is taken complex because the Polyakov loop functional $\Phi[U]$ is complex.

A crucial remark is that, under the center transformation (12), one has

$$\Phi[U^g](\vec{n}) = e^{-i\frac{2\pi}{3}}\Phi[U](\vec{n}), \tag{18}$$

and similarly

$$\Phi[U^{g^\dagger}](\vec{n}) = e^{i\frac{2\pi}{3}}\Phi[U](\vec{n}), \tag{19}$$

which generalizes Eq. (15) for center transformations, and implies

$$\Delta S_W^{\rho,\theta}[U^{g^\dagger}] = \Delta S_W^{\rho,\theta+2\pi/3}[U]. \tag{20}$$

To avoid notation cluttering, here and in what follows, we take the convention that the dagger symbol † has priority over gauge/center transformations, that is, $U^{g^\dagger}$ means the transformation of the link U under the center transformation $g^\dagger$. Were we to represent, instead, the dagger of the transformed link, we would explicitly write $(U^g)^\dagger$.

Having stated these notational conventions, one can now relabel the dummy integration variable in Eq. (17) as $U_\mu(n) \to U_\mu^{g^\dagger}(n)$ with a new configuration $U_\mu(n)$ periodic in all directions. Then, using that the measure and the Wilson action are invariant, whereas the Polyakov loop functional and the perturbation are transformed as in Eqs. (19) and (20), one arrives at

$$\langle\Phi\rangle_{\rho,\theta} = e^{i\frac{2\pi}{3}}\langle\Phi\rangle_{\rho,\theta+2\pi/3}. \tag{21}$$

The fate of this identity as the source $\rho e^{i\theta}$ is sent to 0 depends on whether the Polyakov loop admits a regular limit. For a finite system, the limit is always regular, meaning that $\lim_{\rho\to0^+}\langle\Phi\rangle_{\rho,\theta}$ does not depend on θ. Denoting this common limit as $\langle\Phi\rangle_{\rho\to0^+}$, the identity (21) becomes

$$\langle\Phi\rangle_{\rho\to0^+} = e^{i\frac{2\pi}{3}}\langle\Phi\rangle_{\rho\to0^+}, \tag{22}$$

which implies that $\langle\Phi\rangle_{\rho\to0^+} = 0$. In contrast, for an infinite system, the zero-source limit can be irregular in some range of temperatures. In this case, $\lim_{\rho\to0^+}\langle\Phi\rangle_{\rho,\theta}$ still depends on θ and the identity (21) becomes

$$\langle\Phi\rangle_{\rho\to0^+,\theta} = e^{i\frac{2\pi}{3}}\langle\Phi\rangle_{\rho\to0^+,\theta+2\pi/3}, \tag{23}$$

which does not impose any constraint on the value of $\langle\Phi\rangle_{\rho\to0^+,\theta}$ but rather a relation between the limits for two different values of θ related by the symmetry.

Of course, this second scenario of broken center symmetry never occurs in a finite system in the sense that the function $\langle\Phi\rangle_{\rho,\theta}$ is always continuously connected to 0 as $\rho \to 0^+$. A sufficiently large system, however, can mimic a broken center symmetry behavior, if, for a certain range of

temperatures, the region in ρ where the Polyakov loop approaches 0 becomes extremely small.

C. Lattice implementation

On the lattice, one does not need to introduce a symmetry breaking term to study the breaking of the symmetry. This is rooted in the way in which observables are determined. Let us see how this works.

Recall first that the Polyakov loop is evaluated using a Monte Carlo ensemble $\mathcal{E}$ as

$$\langle\Phi\rangle \simeq \frac{1}{N_{\text{conf}}}\sum_{U\in\mathcal{E}}\Phi[U](\vec{n}) \equiv \langle\Phi(\vec{n})\rangle_{\mathcal{E}}. \tag{24}$$

As we have already mentioned, $\langle\Phi\rangle$ does not depend on $\vec{n}$ due to the translation invariance of the Wilson action and the use of periodic boundary conditions. In practice, this should also be satisfied within errors by the Monte Carlo average $\langle\Phi(\vec{n})\rangle_{\mathcal{E}}$, but there could remain a slight dependence on $\vec{n}$. In this case, it is convenient to evaluate the Polyakov by further averaging over $\vec{n}$:

$$\langle\!\langle\Phi\rangle\!\rangle_{\mathcal{E}} \equiv \frac{1}{L_1L_2L_3}\sum_{\vec{n}}\langle\Phi(\vec{n})\rangle_{\mathcal{E}}. \tag{25}$$

In what follows, we stick to the single average $\langle\Phi\rangle_{\mathcal{E}}$ but all results discussed below apply also to the double average $\langle\!\langle\Phi\rangle\!\rangle_{\mathcal{E}}$.

Let us then denote by $\mathcal{E}^g$ the ensemble of configurations obtained by applying the transformation g to the configurations of the original Monte Carlo ensemble $\mathcal{E}$:

$$\mathcal{E}^g \equiv \{U^g_\mu | U_\mu \in \mathcal{E}\}. \tag{26}$$

This transformed ensemble is just a convenient mathematical construct that allows one to perform a change of variables in Eq. (24). Indeed, it should be clear that the number of configurations in $\mathcal{E}^g$ is the same as in $\mathcal{E}$, and, as U_μ browses the ensemble $\mathcal{E}^g$, $U_\mu^{g^\dagger}$ browses the ensemble $\mathcal{E}$. One can then write

$$\begin{aligned}\langle\Phi\rangle_{\mathcal{E}} &= \frac{1}{N_{\text{conf}}}\sum_{U\in\mathcal{E}^g}\Phi[U^{g^\dagger}](\vec{n})\\ &= \frac{1}{N_{\text{conf}}}\sum_{U\in\mathcal{E}^g}e^{i\frac{2\pi}{3}}\Phi[U](\vec{n})\\ &= \frac{e^{i\frac{2\pi}{3}}}{N_{\text{conf}}}\sum_{U\in\mathcal{E}^g}\Phi[U](\vec{n}) = e^{i\frac{2\pi}{3}}\langle\Phi\rangle_{\mathcal{E}^g},\end{aligned} \tag{27}$$

where we have used Eq. (19). In summary,

$$\langle\Phi\rangle_{\mathcal{E}} = e^{i\frac{2\pi}{3}}\langle\Phi\rangle_{\mathcal{E}^g}, \tag{28}$$

which, to some extent, can be put into correspondence with Eq. (21).

From here, the discussion unfolds according to two possible scenarios:

(i) If the symmetry associated with (12) is not broken dynamically, the Monte Carlo ensemble reflects this symmetry. That is, for most of the configurations $U_\mu(n)$ in $\mathcal{E}$, one can find a configuration close to $U^g_\mu(n)$ and another one close to $U^{g^\dagger}_\mu(n)$. In other words, the Monte Carlo ensemble is approximately invariant under g: $\mathcal{E}^g \simeq \mathcal{E}$. In this case, Eq. (28) becomes

$$\langle\Phi\rangle_{\mathcal{E}} \simeq e^{i\frac{2\pi}{3}}\langle\Phi\rangle_{\mathcal{E}}. \tag{29}$$

This is a constraint on the value taken by $\langle\Phi\rangle_{\mathcal{E}}$ in the symmetric phase, which eventually implies $\langle\Phi\rangle_{\mathcal{E}} \simeq 0$.

(ii) In contrast, if the symmetry is broken spontaneously, the system explores only part of the configurations and there is no reason for $\mathcal{E}$ to be invariant under g, not even approximately: $\mathcal{E}^g \neq \mathcal{E}$. In this case, Eq. (28) is not a constraint on the value of $\langle\Phi\rangle_{\mathcal{E}}$ but rather a relation between the averaged Polyakov loops over two different patches of the configuration space, connected by the transformation (12).

The above discussion shows that the averaged Polyakov loop plays the role of an order parameter for center symmetry. One may advance, however, that this applies only to an infinite system and that, for a finite system, the second scenario, when it applies, just reflects a limitation of the sampling. Indeed, the evolution being ergodic, if one waits long enough, the Monte Carlo ensemble should instead follow the first scenario. Still, a large enough system can mimic the breaking of ergodicity, if, in some range of temperatures, the possibility of transitioning to other regions of the configuration space becomes highly improbable. In this case, the time that would be needed to observe an ensemble complying with the first scenario, although finite, becomes extremely large, larger than any simulation time that one might conceive.

So, even though for finite systems there is strictly speaking no broken center symmetry, if the system is large enough, one may still approach a broken phase behavior, either from the study of how the system reacts to a small symmetry-breaking source or from the nature of the dynamically generated Monte Carlo ensemble.

It should also be noted that, in practice and within a single lattice configuration, the distribution of the Polyakov over the lattice sites differs in the symmetric and broken phases. In particular, for the symmetric phase, the phase of the Polyakov loop is equally distributed among the sectors, so the average over lattice sites favors a vanishing Polyakov loop, and so, even before the ensemble average. On the other hand, in the broken phase, there is a preference for one

of the sectors, hence providing a nonzero Polyakov loop average over the lattice; see [30] for details.

D. Charge conjugation

Let us close this section by recalling that the Wilson action is also invariant under charge conjugation defined on the links as

$$U_\mu(n) \to U_\mu^C(n) \equiv U_\mu^*(n), \tag{30}$$

where the star $*$ denotes complex conjugation. Following a similar reasoning as before, we have

$$\Phi[U^C] = \Phi[U^*] = \Phi[U]^*, \tag{31}$$

and thus that

$$\langle\Phi\rangle_{\mathcal{E}} = \langle\Phi\rangle^*_{\mathcal{E}^C}, \tag{32}$$

where

$$\mathcal{E}^C \equiv \{U_\mu^C | U_\mu \in \mathcal{E}\}. \tag{33}$$

If charge conjugation invariance is not broken, the Monte Carlo ensemble should be approximately invariant under C. In this case, we denote the ensemble by $\mathcal{E}_0$, such that $\mathcal{E}_0^C \simeq \mathcal{E}_0$. The identity (32) then becomes

$$\langle\Phi\rangle_{\mathcal{E}_0} = \langle\Phi\rangle^*_{\mathcal{E}_0}, \tag{34}$$

which implies that $\langle\Phi[U]\rangle_{\mathcal{E}_0}$ is real,[4] in line with its physical interpretation as $e^{-\Delta F/T}$.

Consider now two other ensembles defined by

$$\mathcal{E}_+ \equiv \mathcal{E}_0^{g^\dagger} \quad \text{and} \quad \mathcal{E}_- \equiv \mathcal{E}_0^{g}. \tag{35}$$

In the center-symmetric phase, because $\mathcal{E}_0^g \simeq \mathcal{E}_0$, these ensembles are essentially the same as $\mathcal{E}_0$. In the phase of broken center symmetry, however, they are distinct from $\mathcal{E}_0$ but provide equally valid Monte Carlo ensembles.[5] The ensemble $\mathcal{E}_+$ (respectively, $\mathcal{E}_-$) is not invariant under C but rather under the combined action of g, C, and $g^\dagger$ (respectively, $g^\dagger$, C, and g) which we denote as $g^\dagger \cdot C \cdot g$ (respectively, $g \cdot C \cdot g^\dagger$), where the $\cdot$ refers to the composition of transformations.[6] Indeed,

$$\mathcal{E}_+^{g^\dagger \cdot C \cdot g} \equiv ((\mathcal{E}_+^g)^C)^{g^\dagger} = (\mathcal{E}_0^C)^{g^\dagger} \simeq \mathcal{E}_0^{g^\dagger} = \mathcal{E}_+. \tag{36}$$

Similarly, one shows that $\mathcal{E}_-^{g \cdot C \cdot g^\dagger} \simeq \mathcal{E}_-$.

Now, we write

$$\begin{aligned}\Phi[U^{(g^\dagger \cdot C \cdot g)}] &= \Phi[((U^g)^C)^{g^\dagger}] \\ &= e^{i2\pi/3}\Phi[(U^g)^C] \\ &= e^{i2\pi/3}\Phi[U^g]^* \\ &= e^{i4\pi/3}\Phi[U]^*. \end{aligned} \tag{37}$$

From Eq. (37), one deduces

$$\langle\Phi\rangle_{\mathcal{E}} = e^{i4\pi/3}\langle\Phi\rangle^*_{\mathcal{E}^{g^\dagger \cdot C \cdot g}}, \tag{38}$$

which, for the ensemble $\mathcal{E}_+$ obeying (36), becomes

$$\langle\Phi\rangle_{\mathcal{E}_+} = e^{i4\pi/3}\langle\Phi\rangle^*_{\mathcal{E}_+}, \tag{39}$$

and tells one that the phase of $\langle\Phi\rangle_{\mathcal{E}_+}$ is fixed to $2\pi/3$ modulo π. Of course, a similar reasoning leads to the conclusion that the phase of $\langle\Phi\rangle_{\mathcal{E}_-}$ is fixed to $-2\pi/3$ modulo π.

Deep in the broken phase, the Monte Carlo ensembles will always be of type $\mathcal{E}_0$, $\mathcal{E}_+$, or $\mathcal{E}_-$, and, by applying center transformations, we can always choose to work with an ensemble of type $\mathcal{E}_0$.[7]

IV. LINK CORRELATORS AS ORDER PARAMETERS

We have just recalled why the Polyakov loop average is an observable that plays the role of an order parameter for center symmetry. The two crucial ingredients are, first, that the Polyakov loop functional (14) transforms in a simple (linear) way under the symmetry [see Eq. (18)] and, second, that the Monte Carlo ensemble reflects the symmetry in the symmetric phase, in the sense that $\mathcal{E}^g \simeq \mathcal{E}$ (see the discussion in Sec. III C). In what follows, we would like to construct alternative order parameters from averages of non-gauge-invariant functionals.

A. Link correlators

The basic example of a non-gauge-invariant functional is a tensor product of links

[4]The label 0 in $\mathcal{E}_0$ actually refers to the fact that the phase of the averaged Polyakov loop is 0 in this case.

[5]By this we mean that the configurations in $\mathcal{E}_\pm$ give the same value for the Wilson action as the configurations in $\mathcal{E}_0$.

[6]The need for this notation stems from the fact that, in the SU(3) case, and contrary to the SU(2) case, C is not an element of SU(3) and, therefore, the combination of g, C, and $g^\dagger$ is not just a matrix product in SU(3).

[7]Whenever the system is coupled to dynamical quarks, center symmetry is explicitly broken. In the absence of a baryonic chemical potential, charge conjugation is manifest and the configurations that are favored are those of the type $\mathcal{E}_0$. One way to reach configurations of the type $\mathcal{E}_\pm$ is to introduce an imaginary quark chemical potential equal to $\pm i2\pi/3T$, that is, a baryonic chemical potential equal to $\pm i2\pi T$.

$$U_{\mu_1}(n_1) \otimes \cdots \otimes U_{\mu_p}(n_p), \tag{40}$$

the simplest of which is of course the single link $U_\mu(n)$. These functionals transform linearly under the action of $\mathcal{G}_0$ and $\mathcal{G}$.

It should be stressed, however, that the corresponding averages are usually not defined using the Monte Carlo ensemble $\mathcal{E}$ but, rather, using a gauge-fixed ensemble $\mathcal{E}_{\rm gf}$, which we shall define more precisely below:

$$\begin{aligned}&\langle U_{\mu_1}(n_1) \otimes \cdots \otimes U_{\mu_p}(n_p)\rangle_{\mathcal{E}_{\rm gf}} \\ &\equiv \frac{1}{N_{\rm conf}} \sum_{U\in\mathcal{E}_{\rm gf}} U_{\mu_1}(n_1) \otimes \cdots \otimes U_{\mu_p}(n_p).\end{aligned} \tag{41}$$

Following the same steps as for the Polyakov loop, and exploiting the fact that the links transform linearly under center transformations, one can deduce linear relations obeyed by the link correlators over *a priori* distinct ensembles. For instance, let us work out explicitly the case of the link average. By definition[8]

$$\langle U_\mu(n)\rangle_{\mathcal{E}_{\rm gf}} \equiv \frac{1}{N_{\rm conf}} \sum_{U\in\mathcal{E}_{\rm gf}} U_\mu(n), \tag{42}$$

and, as for the Polyakov loop, we can combine the ensemble average with a lattice average

$$\langle\!\langle U_\mu\rangle\!\rangle_{\mathcal{E}_{\rm gf}} \equiv \frac{1}{L_1L_2L_3L_4} \sum_n \langle U_\mu(n)\rangle_{\mathcal{E}_{\rm gf}}. \tag{43}$$

We now denote by $\mathcal{E}^g_{\rm gf}$ the ensemble of configurations obtained by applying the transformation g to the configurations of the original gauge-fixed ensemble $\mathcal{E}_{\rm gf}$:

$$\mathcal{E}^g_{\rm gf} = \{U^g_\mu | U_\mu \in \mathcal{E}_{\rm gf}\}. \tag{44}$$

It should be clear that $\mathcal{E}_{\rm gf}$ and $\mathcal{E}^g_{\rm gf}$ contain the same number of configurations and that, as U_μ browses $\mathcal{E}^g_{\rm gf}$, $U^{g^\dagger}_\mu$ browses $\mathcal{E}_{\rm gf}$. One can then write

$$\begin{aligned}\langle U_\mu(n)\rangle_{\mathcal{E}_{\rm gf}} &= \frac{1}{N_{\rm conf}} \sum_{U\in\mathcal{E}^g_{\rm gf}} U^{g^\dagger}_\mu(n) \\ &= \frac{1}{N_{\rm conf}} \sum_{U\in\mathcal{E}^g_{\rm gf}} g^\dagger(n) U_\mu(n) g(n+\hat\mu) \\ &= g^\dagger(n)\left[\frac{1}{N_{\rm conf}} \sum_{U\in\mathcal{E}^g_{\rm gf}} U_\mu(n)\right] g(n+\hat\mu),\end{aligned} \tag{45}$$

and thus

$$\langle U_\mu(n)\rangle_{\mathcal{E}_{\rm gf}} = g^\dagger(n)\langle U_\mu(n)\rangle_{\mathcal{E}^g_{\rm gf}} g(n+\hat\mu). \tag{46}$$

Similar relations can be deduced for higher link correlators.

All these relations look rather similar to Eq. (28), and then, it is tempting to deduce that the link correlators can play the role of order parameters for center symmetry. However, the possibility to use these quantities as order parameters relies on whether, in the symmetric phase, the ensemble $\mathcal{E}^g_{\rm gf}$ that appears in the right-hand side (RHS) of (46) is approximately equal to the gauge-fixed ensemble $\mathcal{E}_{\rm gf}$ that appears in the left-hand side (LHS).

As we now argue, for generic gauges, $\mathcal{E}_{\rm gf}$ and $\mathcal{E}^g_{\rm gf}$ are distinct, even in the symmetric phase, as they correspond to gauge-fixed ensembles in different gauges. In this case, Eq. (46) relates the link average in two different gauges but in no way can it fix the value of the link average in any of the two gauges. For specific types of gauges, however, and for specific associated center transformations $\tilde g$, the ensembles $\mathcal{E}_{\rm gf}$ and $\mathcal{E}^{\tilde g}_{\rm gf}$ are made of link configurations in the same gauge. Moreover, for specific choices of the Gribov copies that are potentially present in those gauges, the ensembles $\mathcal{E}_{\rm gf}$ and $\mathcal{E}^{\tilde g}_{\rm gf}$ are approximately equal in the symmetric phase. In this case, Eq. (46), for the specific choice of center transformation $\tilde g$, becomes a constraint for the link average in that gauge, which then becomes a potential order parameter for center symmetry.

B. Gauge fixing

Before proceeding with the proof, let us recall how the gauge fixing is implemented on the lattice.

A given gauge is specified by the choice of a functional $F[U]$ defined over the link configurations. A gauge fixing within that gauge is obtained by replacing each configuration $U_\mu \in \mathcal{E}$ of the original Monte Carlo ensemble by a local maximum of $F[U]$ along the $\mathcal{G}_0$-orbit of U_μ. In other words, for any fixed $U_\mu \in \mathcal{E}$, one looks for a local maximum of the function $g_0 \mapsto F[U^{g_0}]$ over $\mathcal{G}_0$. By construction, the gauge-fixed configurations $U_\star$ are such that

$$F[U^{g_0}_\star] < F[U_\star], \tag{47}$$

for any $g_0 \in \mathcal{G}_0$ close to the identity transformation.

It is important to keep in mind that the maximization is done along the $\mathcal{G}_0$-orbits and not along the $\mathcal{G}$-orbits. This is because, despite the fact that the transformations in $\mathcal{G}$ write mathematically as gauge transformations, they correspond to actual physical symmetries, and not redundancies of the description in terms of gauge fields. Nevertheless, it will be important below to study the transformation properties of $F[U]$ under the action of $\mathcal{G}$. This will naturally lead us to consider $F[U^g]$ for $g \in \mathcal{G}$.

[8]Note that, in general, the average of SU(3) matrices is not a SU(3) matrix.

There are some restrictions on the functional $F[U]$. First, it should not be invariant under the action of $\mathcal{G}_0$; otherwise, there are no local maxima (or all configurations are degenerate maxima) and gauge fixing is not possible. Second, there should be at least one maximum per $\mathcal{G}_0$-orbit. In fact, it is very often the case that there are actually many local maxima along each $\mathcal{G}_0$-orbit, known as Gribov copies. In this case, there exist various possible gauge fixings in a given gauge, depending on which copy is selected on each orbit. In what follows, we denote generically by $\mathcal{E}_{\rm gf}$ any such choice of copies along the orbits of the link configurations in the original Monte Carlo ensemble $\mathcal{E}$.

C. Generic gauge

We first consider a generic gauge,[9] associated with a functional $F[U]$. Given a gauge-fixed ensemble $\mathcal{E}_{\rm gf}$ in this gauge, we would like to argue that the transformed ensemble $\mathcal{E}^g_{\rm gf}$ corresponds to a gauge-fixed ensemble in a different gauge, and thus that the two ensembles cannot coincide in this generic setting, not even in the center-symmetric phase.

To this aim, let us show that the transformed ensemble $\mathcal{E}^g_{\rm gf}$ that enters Eq. (46) is made of all the configurations that maximize the functional $F[U^{g^\dagger}]$ (seen as a functional of U for a fixed g) along the $\mathcal{G}_0$-orbits of $\mathcal{E}^g$. To see this, consider a configuration $U_\star$ that maximizes $F[U]$ [see Eq. (47)], and let us evaluate $F[U^{g^\dagger}]$ in the vicinity of $U^g_\star$ along its $\mathcal{G}_0$-orbit. This means that we have to evaluate

$$F[((U^g_\star)^{g_0})^{g^\dagger}] = F[U^{g^\dagger g_0 g}_\star]. \tag{48}$$

Now, because $\tilde{g}_0 \equiv g^\dagger g_0 g$ is periodic and close to the identity,[10] we can use Eq. (47) to deduce that

$$F[((U^g_\star)^{g_0})^{g^\dagger}] = F[U^{\tilde{g}_0}_\star] < F[U_\star] = F[(U^g_\star)^{g^\dagger}], \tag{49}$$

for g_0 close to the identity. This shows that the configurations of $\mathcal{E}^g_{\rm gf}$ are (local) maxima of the functional $F[U^{g^\dagger}]$ along the $\mathcal{G}_0$-orbits of $\mathcal{E}^g$.

But for a generic choice of gauge, the functional $F[U^{g^\dagger}]$ has no reason to be equal to the original one $F[U]$. Then, the configurations in $\mathcal{E}_{\rm gf}$ and in $\mathcal{E}^g_{\rm gf}$ are configurations in two distinct gauges. In this case, as already stated above, the identity (46) merely relates the correlators in these two gauges but in no way constrains their values in any of these gauges. For this reason, the link correlators in a generic gauge are not order parameters for center symmetry.

Note that this conclusion applies to correlators evaluated over a given ensemble. However, this does not prevent one from constructing order parameters by comparing the correlators evaluated over different ensembles. One example of such construction in the standard Landau gauge is that of Ref. [29] where order parameters are constructed by comparing the propagators over distinct center sectors. We leave the comparison between the present approach and the one in Ref. [29] for a future work.

Note also that, even though the gauge-fixed ensemble $\mathcal{E}_{\rm gf}$ in a generic gauge is not invariant under any given center transformation g in the symmetric phase, it still contains information about center symmetry. Indeed, given $U \in \mathcal{E}_{\rm gf}$, U^g is in general not in $\mathcal{E}_{\rm gf}$, but it is possible to find a $g_0 \in \mathcal{G}_0$ such that $(U^g)^{g_0} = U^{g_0 g}$ is back in $\mathcal{E}_{\rm gf}$ and thus $\mathcal{E}^{g_0 g}_{\rm gf} \simeq \mathcal{E}_{\rm gf}$. One could then wonder what prevents one from repeating the same steps that lead to (46) using $g_0 g$ instead of g and, given that $\mathcal{E}^{g_0 g}_{\rm gf} \simeq \mathcal{E}_{\rm gf}$, to obtain a center symmetry constraint in a generic gauge. The loophole is that, *a priori*, the transformation g_0 depends on U and then so does $g_0 g$. This prevents one from completing the last steps in (45) simply because the configuration-dependent transformation $g_0 g$ cannot be pulled out of the sum over all configurations. This problem can be overcome by using the class of center-symmetric gauges that we now discuss.

D. Center-symmetric gauges

Suppose that we were able to find a particular type of functionals $\tilde{F}[U]$ invariant under certain representatives $\tilde{g} \in \mathcal{G}$ of the center transformations[11]

$$\tilde{F}[U^{\tilde{g}}] = \tilde{F}[U]. \tag{50}$$

We dub these functionals, and the associated gauges, as center-symmetric. We shall construct one explicit example in Sec. V.

The discussion in the previous section applies here too, so the configurations in $\mathcal{E}^{\tilde{g}}_{\rm gf}$ maximize the functional $\tilde{F}[U^{\tilde{g}^\dagger}]$ along the $\mathcal{G}_0$-orbits of $\mathcal{E}^{\tilde{g}}$. But from Eq. (50), it follows that the functional $\tilde{F}[U^{\tilde{g}^\dagger}]$ is nothing but the original functional $\tilde{F}[U]$. We deduce from this that, in a center-symmetric gauge, and contrary to the case of a generic gauge, the

[9] By generic, we mean that we do not assume any special properties of the functional $F[U]$ other than the minimal ones listed above.

[10] The periodicity along the spatial directions is trivial. Along the temporal direction, we write

$$\begin{aligned}\tilde{g}_0(n+L_4\hat{4}) &= g^\dagger(n+L_4\hat{4})g_0(n+L_4\hat{4})g(n+L_4\hat{4}) \\ &= e^{-i2\pi/3}g^\dagger(n)g_0(n)g(n)e^{i2\pi/3} = g^\dagger(n)g_0(n)g \\ &= \tilde{g}_0(n).\end{aligned}$$

[11] Because the Wilson action is invariant under genuine gauge transformations g_0, there are infinitely many ways to define the center transformations: a center transformation g is physically undistinguishable from $g_0 g$. In a gauge-fixed setting, in contrast, when center symmetry is manifest, it is so only for certain representatives $g_0 g$.

configurations in $\mathcal{E}_{\rm gf}$ and $\mathcal{E}_{\rm gf}^{\tilde{g}}$ maximize the same functional (along *a priori* distinct orbits for the moment) and thus correspond to configurations in the same gauge.

Consider now the symmetric phase for which $\mathcal{E}^{\tilde{g}} \simeq \mathcal{E}$. In this case, not only do the configurations in $\mathcal{E}_{\rm gf}$ and $\mathcal{E}_{\rm gf}^{\tilde{g}}$ maximize the same functional, but they do so along the same orbits, those of $\mathcal{E}^{\tilde{g}} \simeq \mathcal{E}$. If we assume for the moment that $\tilde{F}[U]$ is such that there are no Gribov copies, then we deduce that $\mathcal{E}_{\rm gf}^{\tilde{g}} \simeq \mathcal{E}_{\rm gf}$. In this case, the identity (46), for the specific choice $g \to \tilde{g}$, becomes a constraint for the link correlator in the center-symmetric gauge[12]:

$$\langle U_\mu(n)\rangle_{\mathcal{E}_{\rm gf}} = \tilde{g}^\dagger(n)\langle U_\mu(n)\rangle_{\mathcal{E}_{\rm gf}}\tilde{g}(n+\hat{\mu}). \tag{51}$$

This constraint fixes the value of the correlator (or of some of its components) in the symmetric phase which thus turns into a potential order parameter for center symmetry.[13]

Note also that in the broken phase, we will have $\mathcal{E}_{\rm gf}^{\tilde{g}}$ distinct from $\mathcal{E}_{\rm gf}$, but, as we already pointed out above, contrary to what happens in the generic case, here these two ensembles contain configurations in the same gauge. These ensembles can be interpreted as distinct center symmetry broken states connected by the symmetry.

E. Gribov copies

Let us now see how the discussion extends in the presence of Gribov copies. Of course, it could be that the quantity that we want to put forward as an order parameter is not much affected by the choice of copies, in which case the discussion in the previous section applies and the gauge-fixed ensemble can be assumed to be approximately $\tilde{g}$-invariant in the symmetric phase.

In the case where the choice of copies has a non-negligible impact on the quantity of interest, the discussion is slightly more subtle. Indeed, the fact that the ensembles $\mathcal{E}_{\rm gf}$ and $\mathcal{E}_{\rm gf}^{\tilde{g}}$ maximize the same functional along the same orbits is not enough to conclude that $\mathcal{E}_{\rm gf}^{\tilde{g}} \simeq \mathcal{E}_{\rm gf}$. This very property, and thus the possibility of deriving (51) and of using the link average as an order parameter, depends crucially on the way the copies are chosen. Stated differently, in this case, having a center-symmetric gauge does not imply necessarily that the gauge fixing is center symmetric.

Consider first the ideal situation of absolute gauge fixing where the functional $\tilde{F}[U]$ is assumed to have only one absolute maximum per gauge orbit and that this is the maximum selected to form the gauge-fixed ensemble. Since the configurations in $\mathcal{E}_{\rm gf}$ and $\mathcal{E}_{\rm gf}^{\tilde{g}}$ absolutely maximize the functional $\tilde{F}[U]$ along the same orbits, those of $\mathcal{E}^{\tilde{g}} \simeq \mathcal{E}$ in the symmetric phase, and because the absolute maximum is assumed to be unique along each $\mathcal{G}_0$-orbit, we deduce that $\mathcal{E}_{\rm gf}^{\tilde{g}} \simeq \mathcal{E}_{\rm gf}$ in the symmetric phase. So maximal gauge fixing in a center-symmetric gauge is itself center-symmetric.

Unfortunately, such type of gauge fixing is difficult, if not impossible to implement in practice and the lattice approach resorts instead to choosing one local maximum of the gauge-fixed functional per $\mathcal{G}_0$-orbit (this is sometimes referred to as "minimal" gauge fixing). The search for maxima is typically done using algorithms based on the steepest ascent method. In Appendix D, we show that, in the case of a center-symmetric gauge $\tilde{F}[U]$, the most primitive version of such algorithms is symmetry preserving: applying it to two configurations U and $U^{\tilde{g}}$ related by a transformation $\tilde{g}$ that leaves $\tilde{F}[U]$ invariant, it gives maxima on the $\mathcal{G}_0$-orbits of U and $U^{\tilde{g}}$ that are themselves related by $\tilde{g}$. This ensures that $\mathcal{E}_{\rm gf}^{\tilde{g}} \simeq \mathcal{E}_{\rm gf}$.

In practice, however, this basic steepest ascent algorithm is upgraded using various acceleration routines which may destroy this symmetry preserving property, at least partially. It is of interest to investigate the possibility of constructing explicit symmetry preserving algorithms. However, we note that this may not be really necessary for practical purposes. Here is the argument.

Indeed, as we have already stressed, the Monte Carlo ensemble is generated using the Wilson action which is gauge-invariant, and, because gauge invariance cannot break dynamically, the configurations of the Monte Carlo ensemble can be grouped in subsets of configurations that are almost along the same orbits. Then, even though $\mathcal{E}_{\rm gf}$ is obtained by selecting one copy per orbit, the configurations forming this ensemble can be grouped in subsets of configurations that are almost Gribov copies of each other. This clearly increases the possibility that, in the symmetric phase, some fraction of the selected maxima are approximately pairwise related by the transformation $\tilde{g}$ defined in Eq. (50). Note that this is true irrespectively of whether we construct the gauge-fixed ensemble in the center-symmetric gauge starting from a genuine Monte Carlo ensemble or from any other gauge-fixed ensemble in a generic gauge. This is because, as we have already mentioned, gauge-fixed ensembles in generic gauges still contain the information about center symmetry although this information might be hidden behind a configuration-dependent center transformation.

Note finally that this second argument applies strictly speaking in the scenario where the Monte Carlo ensemble is sufficiently large. In practice, the ensemble is of a moderate size, and the above expectation applies only with some degree of approximation. At the end of the day, the best that

[12]Strictly speaking, this is an approximate equality since $\mathcal{E}_{\rm gf}^{\tilde{g}}$ is only approximately equal to $\mathcal{E}_{\rm gf}$ due to the finite sample size.

[13]Of course, there is still the possibility that the correlator also receives stronger constraints from other, unbroken symmetries, in which case it might not be possible to use it as a probe for center symmetry.

can be done regarding the question of whether $\mathcal{E}^{\tilde{g}}_{\rm gf} \simeq \mathcal{E}_{\rm gf}$ in the symmetric phase is to verify numerically that, for a given choice of copies, the consequences of $\mathcal{E}^{\tilde{g}}_{\rm gf} \simeq \mathcal{E}_{\rm gf}$, such as Eq. (51), are realized, and also to try to quantify how much $\mathcal{E}^{\tilde{g}}_{\rm gf}$ resembles $\mathcal{E}_{\rm gf}$. These two complementary aspects will be discussed below, in Secs. V E and VI C, respectively.

V. THE CENTER-SYMMETRIC LANDAU GAUGE

After these general considerations, let us now construct an explicit example of a center-symmetric gauge on the lattice.

A. Preamble

In what follows, we denote the Gell-Mann matrices by λ_a, with $a = 1, \ldots, 8$:

$$\lambda_1 = \begin{pmatrix} 0 & 1 & 0 \\ 1 & 0 & 0 \\ 0 & 0 & 0 \end{pmatrix}, \qquad \lambda_2 = \begin{pmatrix} 0 & -i & 0 \\ i & 0 & 0 \\ 0 & 0 & 0 \end{pmatrix},$$
$$\lambda_4 = \begin{pmatrix} 0 & 0 & 1 \\ 0 & 0 & 0 \\ 1 & 0 & 0 \end{pmatrix}, \qquad \lambda_5 = \begin{pmatrix} 0 & 0 & -i \\ 0 & 0 & 0 \\ i & 0 & 0 \end{pmatrix},$$
$$\lambda_6 = \begin{pmatrix} 0 & 0 & 0 \\ 0 & 0 & 1 \\ 0 & 1 & 0 \end{pmatrix}, \qquad \lambda_7 = \begin{pmatrix} 0 & 0 & 0 \\ 0 & 0 & -i \\ 0 & i & 0 \end{pmatrix},$$
$$\lambda_3 = \begin{pmatrix} 1 & 0 & 0 \\ 0 & -1 & 0 \\ 0 & 0 & 0 \end{pmatrix}, \qquad \lambda_8 = \frac{1}{\sqrt{3}} \begin{pmatrix} 1 & 0 & 0 \\ 0 & 1 & 0 \\ 0 & 0 & -2 \end{pmatrix}. \tag{52}$$

From those, we shall be forming two color rotations

$$e^{i\pi\frac{\lambda_1}{2}} = \begin{pmatrix} 0 & i & 0 \\ i & 0 & 0 \\ 0 & 0 & 1 \end{pmatrix}, \qquad e^{i\pi\frac{\lambda_4}{2}} = \begin{pmatrix} 0 & 0 & i \\ 0 & 1 & 0 \\ i & 0 & 0 \end{pmatrix}, \tag{53}$$

and a center transformation

$$e^{-i\frac{n_4}{L_4}\pi(\lambda_3+\frac{\lambda_8}{\sqrt{3}})} = \begin{pmatrix} e^{-i\frac{4\pi n_4}{3L_4}} & 0 & 0 \\ 0 & e^{i\frac{2\pi n_4}{3L_4}} & 0 \\ 0 & 0 & e^{i\frac{2\pi n_4}{3L_4}} \end{pmatrix}. \tag{54}$$

That the latter is a center transformation is easily checked as a shift of n_4 by L_4 just produces an overall phase $e^{-i4\pi/3} = e^{i2\pi/3}$. We also note that any product of this particular center transformation with the two color rotations given above is also a center transformation associated with the same phase.

Consider now a 3×3 diagonal matrix X. It is easily checked that the adjoint action of $e^{i\pi\frac{\lambda_1}{2}}$ on X is to flip the first and second lines and the first and second columns of X and thus to exchange X_{11} and X_{22}:

$$e^{i\pi\frac{\lambda_1}{2}} \begin{pmatrix} X_{11} & 0 & 0 \\ 0 & X_{22} & 0 \\ 0 & 0 & X_{33} \end{pmatrix} e^{-i\pi\frac{\lambda_1}{2}} = \begin{pmatrix} X_{22} & 0 & 0 \\ 0 & X_{11} & 0 \\ 0 & 0 & X_{33} \end{pmatrix}. \tag{55}$$

Similarly, the adjoint action of $e^{i\pi\frac{\lambda_4}{2}}$ corresponds to permuting X_{11} and X_{33}:

$$e^{i\pi\frac{\lambda_4}{2}} \begin{pmatrix} X_{11} & 0 & 0 \\ 0 & X_{22} & 0 \\ 0 & 0 & X_{33} \end{pmatrix} e^{-i\pi\frac{\lambda_4}{2}} = \begin{pmatrix} X_{33} & 0 & 0 \\ 0 & X_{22} & 0 \\ 0 & 0 & X_{11} \end{pmatrix}. \tag{56}$$

Finally, it is easily checked that the center transformation (54) acts on X by multiplying the diagonal elements by the appropriate phases:

$$e^{-i\frac{n_4}{L_4}\pi(\lambda_3+\frac{\lambda_8}{\sqrt{3}})} \begin{pmatrix} X_{11} & 0 & 0 \\ 0 & X_{22} & 0 \\ 0 & 0 & X_{33} \end{pmatrix} e^{i\frac{n_4+\hat{\mu}_4}{L_4}\pi(\lambda_3+\frac{\lambda_8}{\sqrt{3}})}$$
$$= \begin{pmatrix} e^{i\frac{4\pi\hat{\mu}_4}{3L_4}} X_{11} & 0 & 0 \\ 0 & e^{-i\frac{2\pi\hat{\mu}_4}{3L_4}} X_{22} & 0 \\ 0 & 0 & e^{-i\frac{2\pi\hat{\mu}_4}{3L_4}} X_{33} \end{pmatrix}. \tag{57}$$

B. Constructing a center-symmetric functional

Consider now the following class of gauge-fixing functionals:

$$F_X[U] \equiv \sum_{n,\mu} \mathrm{Re\,tr}[X^\dagger U_\mu(n)], \tag{58}$$

parametrized by a diagonal 3×3 matrix X. This is an extension of the Landau gauge functional which corresponds to the choice $X = \mathbb{1}$.

Under a generic center transformation, the functional transforms as

$$F_X[U^g] = \sum_{n,\mu} \mathrm{Re\,tr}[X^\dagger g(n) U_\mu(n) g^\dagger(n+\hat{\mu})]$$
$$= \sum_{n,\mu} \mathrm{Re\,tr}[g^\dagger(n+\hat{\mu}) X^\dagger g(n) U_\mu(n)]. \tag{59}$$

We thus see that a sufficient condition for the functional to be center-invariant is to find particular instances $\tilde{X}$ and $\tilde{g}$ of X and g such that

$$\tilde{g}^\dagger(n+\hat{\mu})\tilde{X}^\dagger\tilde{g}(n)=\tilde{X}^\dagger, \tag{60}$$

or, equivalently,

$$\tilde{g}(n)\tilde{X}\tilde{g}^\dagger(n+\hat{\mu})=\tilde{X}. \tag{61}$$

Note that $\tilde{X}=\mathbb{1}$ cannot be a good candidate since $\tilde{g}(n)$ would need to satisfy $\tilde{g}(n)\tilde{g}^\dagger(n+\hat{\mu})=\mathbb{1}$ for any n and any $\hat{\mu}$, that is, $\tilde{g}(n)$ would have to be a constant, at odds with the fact that it is periodic along the temporal direction modulo a center element. Thus, $\tilde{X}$ needs to have a nontrivial structure. Moreover, the center transformation $\tilde{g}(n)$ cannot be chosen to be the one in the previous section [see Eq. (57)] because its action on X amounts to a phase multiplication of the diagonal elements. The only diagonal matrix invariant under that transformation is $X=0$ but this does not lead to a sensible gauge-fixing functional.

However, we can now combine the center transformation (54) with the color rotations in Eq. (53) to form another center transformation:

$$\tilde{g}(n)=e^{i\pi\frac{\lambda_4}{2}}e^{i\pi\frac{\lambda_1}{2}}e^{-i\frac{n_4}{L_4}\pi(\lambda_3+\frac{\lambda_8}{\sqrt{3}})}. \tag{62}$$

According to Eqs. (55)–(57), we now have

$$\begin{aligned}\tilde{g}(n)&\begin{pmatrix}\tilde{X}_{11}&0&0\\0&\tilde{X}_{22}&0\\0&0&\tilde{X}_{33}\end{pmatrix}\tilde{g}^\dagger(n+\hat{\mu})\\&=\begin{pmatrix}e^{-i\frac{2\pi}{3}\frac{\hat{\mu}_4}{L_4}}\tilde{X}_{33}&0&0\\0&e^{i\frac{4\pi}{3}\frac{\hat{\mu}_4}{L_4}}\tilde{X}_{11}&0\\0&0&e^{-i\frac{2\pi}{3}\frac{\hat{\mu}_4}{L_4}}\tilde{X}_{22}\end{pmatrix}.\end{aligned} \tag{63}$$

The looked after matrix $\tilde{X}$ is then such that

$$\tilde{X}_{11}=e^{-i\frac{2\pi}{3}\frac{\hat{\mu}_4}{L_4}}\tilde{X}_{33}, \tag{64}$$

$$\tilde{X}_{22}=e^{i\frac{4\pi}{3}\frac{\hat{\mu}_4}{L_4}}\tilde{X}_{11}, \tag{65}$$

$$\tilde{X}_{33}=e^{-i\frac{2\pi}{3}\frac{\hat{\mu}_4}{L_4}}\tilde{X}_{22}. \tag{66}$$

The third equation being trivially satisfied once the other two are, this leaves us with the general solution

$$\tilde{X}_{11}=\eta e^{-i\frac{2\pi}{3}\frac{\hat{\mu}_4}{L_4}}, \tag{67}$$

$$\tilde{X}_{22}=\eta e^{i\frac{2\pi}{3}\frac{\hat{\mu}_4}{L_4}}, \tag{68}$$

in terms of an arbitrary complex number $\tilde{X}_{33}=\eta$. In other words, the looked-after matrix $\tilde{X}$ has the structure

$$\tilde{X}=\eta e^{-i\frac{4\pi}{3}\frac{\hat{\mu}_4}{L_4}\frac{\lambda_3}{2}}. \tag{69}$$

Contrary to the choice $\eta=0$ mentioned above, choosing $\eta=1$ leads to a meaningful gauge-fixing functional:

$$\tilde{F}[U]\equiv\sum_{n,\mu}\mathrm{Re\,tr}[e^{i\frac{4\pi}{3}\frac{\hat{\mu}_4}{L_4}\frac{\lambda_3}{2}}U_\mu(n)], \tag{70}$$

which, by construction, is invariant under the center transformation (62). We refer to this functional as the center-symmetric Landau gauge functional. Its relation with the center-symmetric Landau gauge defined in the continuum is analyzed in Appendix A.

C. Other symmetries

The center-symmetric Landau gauge (70) functional benefits from additional invariance properties that constrain the structure of the link correlators.

First, as it can trivially be checked, the functional $\tilde{F}[U]$ is invariant under global color rotations of the form

$$U_\mu(n)\to e^{i\theta^j t^j}U_\mu(n)e^{-i\theta^j t^j}\equiv U^\theta_\mu(n), \tag{71}$$

where the t^j denote the commuting generators of the algebra, here $\lambda_3/2$ and $\lambda_8/2$.

Second, it is invariant (and so is the Wilson action) under the transformation

$$U_\mu(n)\to e^{i\pi\frac{\lambda_1}{2}}U^*_\mu(n)e^{-i\pi\frac{\lambda_1}{2}}\equiv U^{\hat{C}}_\mu(n), \tag{72}$$

which combines charge conjugation as defined in Eq. (30) and a particular color rotation (known as Weyl transformation).[14] When applied to a diagonal matrix, this transformation reads

$$e^{i\pi\frac{\lambda_1}{2}}\begin{pmatrix}X_{11}&0&0\\0&X_{22}&0\\0&0&X_{33}\end{pmatrix}^*e^{-i\pi\frac{\lambda_1}{2}}=\begin{pmatrix}X^*_{22}&0&0\\0&X^*_{11}&0\\0&0&X^*_{33}\end{pmatrix}. \tag{73}$$

Now

[14] As any other physical symmetry, the action of charge conjugation on gauge-dependent objects, such as links, is defined modulo a gauge transformation, so $U_\mu(n)\to U^*_\mu(n)$ or $U_\mu(n)\to g_0(n)U^*_\mu(n)g_0^\dagger(n+\hat{\mu})$ are equally good definitions of charge conjugation, in the sense that they act equally on observables. In a gauge-fixed setting, it might be useful to consider one particular realization, in particular if it leaves the gauge-fixing functional invariant. This is what we have done here.

$$\begin{aligned}\tilde{F}[U^{\hat{C}}] &= \sum_{n,\mu} \mathrm{Re\,tr} e^{i\frac{4\pi}{3}\frac{\hat{\mu}_4}{L_4}\frac{\lambda_3}{2}} e^{i\pi\frac{\lambda_1}{2}} U_\mu^*(n) e^{-i\pi\frac{\lambda_1}{2}} \\ &= \sum_{n,\mu} \mathrm{Re\,tr} e^{-i\frac{4\pi}{3}\frac{\hat{\mu}_4}{L_4}\frac{\lambda_3}{2}} e^{-i\pi\frac{\lambda_1}{2}} U_\mu(n) e^{i\pi\frac{\lambda_1}{2}} \\ &= \sum_{n,\mu} \mathrm{Re\,tr} e^{i\pi\frac{\lambda_1}{2}} e^{-i\frac{4\pi}{3}\frac{\hat{\mu}_4}{L_4}\frac{\lambda_3}{2}} e^{-i\pi\frac{\lambda_1}{2}} U_\mu(n), \end{aligned} \tag{74}$$

so it all boils down to showing that

$$e^{i\pi\frac{\lambda_1}{2}} e^{-i\frac{4\pi}{3}\frac{\hat{\mu}_4}{L_4}\frac{\lambda_3}{2}} e^{-i\pi\frac{\lambda_1}{2}} = e^{i\frac{4\pi}{3}\frac{\hat{\mu}_4}{L_4}\frac{\lambda_3}{2}}. \tag{75}$$

For $\mu \neq 4$, this is obvious. For $\mu = 4$, this follows from Eq. (73).

Let us stress that the Monte Carlo ensembles of type $\mathcal{E}_0$ (see the discussion in Sec. III D), which are approximately invariant under C defined in Eq. (30), are also approximately invariant under $\hat{C}$ defined in Eq. (72). This is because, a Monte Carlo ensemble should always be approximately invariant under genuine gauge transformation, and thus, in particular, under global color rotations. Since the connection between C and $\hat{C}$ is precisely a global color rotation, we deduce that $\mathcal{E}_0$ should also be invariant under $\hat{C}$.

Now, using that the center-symmetric Landau gauge functional $\tilde{F}[U]$ is invariant under $\hat{C}$, and using a similar reasoning as the one done above for the invariance under $\tilde{g}$, we deduce that for appropriately chosen copies, the gauge-fixed ensemble $\mathcal{E}_{0\mathrm{gf}}$ is invariant under $\hat{C}$. This remark is important because it implies that, as long as we do our gauge-fixing starting from an ensemble of type $\mathcal{E}_0$, we will be able to use the constraints associated with the symmetry $\hat{C}$ (see below).

Now, suppose we wanted to do the gauge-fixing starting from the Monte Carlo ensembles $\mathcal{E}_+ = \mathcal{E}_0^{\tilde{g}^\dagger}$ or $\mathcal{E}_- = \mathcal{E}_0^{\tilde{g}}$, see Sec. III D. The first good news is that it is very simple to do so in the center-symmetric Landau gauge, because one just needs to consider as gauge-fixed ensembles $\mathcal{E}_{+\mathrm{gf}} \equiv \mathcal{E}_{0\mathrm{gf}}^{\tilde{g}^\dagger}$ and $\mathcal{E}_{-\mathrm{gf}} \equiv \mathcal{E}_{0\mathrm{gf}}^{\tilde{g}}$. Indeed, unlike what would happen in a generic gauge, these ensembles contain configurations in the same center-symmetric gauge as $\mathcal{E}_{0\mathrm{gf}}$. Moreover, the configurations in $\mathcal{E}_{\pm\mathrm{gf}}$ lie along the $\mathcal{G}_0$-orbits of the configurations in $\mathcal{E}_\pm$. These gauge-fixed ensembles are not approximately invariant under $\hat{C}$, but following similar steps as those in Sec. III D, it is easily argued that they are approximately invariant under $\tilde{g}^\dagger \cdot \hat{C} \cdot \tilde{g}$ and $\tilde{g} \cdot \hat{C} \cdot \tilde{g}^\dagger$, respectively.

D. Link average

We are now fully equipped to derive center symmetry constraints on the link average computed in the center-symmetric Landau gauge. In what follows, we slightly simplify the notation by dropping the reference to the gauge-fixing ensemble in the definition of the average:

$$\langle U_\mu(n)\rangle_{\mathcal{E}_{\mathrm{gf}}} \to \langle U_\mu(n)\rangle. \tag{76}$$

According to the general discussion, if center symmetry is not broken by the gauge-fixed ensemble, we should have

$$\langle U_\mu(n)\rangle = \tilde{g}(n)\langle U_\mu(n)\rangle\tilde{g}^\dagger(n+\hat{\mu}). \tag{77}$$

This is a constraint on the possible values of the local link average in the symmetric phase, just as Eq. (29) is a constraint for the value of the Polyakov loop in the symmetric phase.

The question is now what are the possible values for $\langle U_\mu(n)\rangle$ in the symmetric phase? To answer this question, we note that, from color invariance (71), the 3×3 matrix $\langle U_\mu(n)\rangle$ is diagonal. This is exactly the same problem as the one discussed in the previous section to identify the possible $\tilde{X}$. We deduce that

$$\langle U_\mu(n)\rangle = \eta e^{-i\frac{4\pi}{3}\frac{\mu_4}{L_4}\frac{\lambda_3}{2}}, \tag{78}$$

for some $\eta \in \mathbb{C}$. We have thus shown that, up to a numerical prefactor η,[15] the matrix structure of $\langle U_\mu(n)\rangle$ is entirely fixed in the center-symmetric phase.

In particular, for a temporal link average in the symmetric phase we find[16]

$$\langle U_4(n)\rangle = \eta \begin{pmatrix} e^{-i\frac{2\pi}{3L_4}} & 0 & 0 \\ 0 & e^{i\frac{2\pi}{3L_4}} & 0 \\ 0 & 0 & 1 \end{pmatrix}. \tag{79}$$

We will see below that $\eta \in \mathbb{R}$ and, because $\det\langle U_4(n)\rangle = \eta^3$, we can rewrite Eq. (79) as

$$\frac{\langle U_4(n)\rangle}{(\det\langle U_4(n)\rangle)^{1/3}} = \begin{pmatrix} e^{-i\frac{2\pi}{3L_4}} & 0 & 0 \\ 0 & e^{i\frac{2\pi}{3L_4}} & 0 \\ 0 & 0 & 1 \end{pmatrix}. \tag{80}$$

[15]Because the elements of a unitary matrix have moduli bounded by 1, so is the case of the elements of the average. From this we deduce that $|\eta| \leq 1$. We will show below that $\eta \in \mathbb{R}$.

[16]As before, the fact that the link average does not depend on n is a consequence of translation invariance, which holds true owing to the translation invariance of the Wilson action and the use of periodic boundary conditions. Within a given Monte Carlo evaluation of the link average there will remain a spurious dependence on n. In this case, it might be convenient to define the link average by further averaging over the lattice sites

$$\langle\langle U_4\rangle\rangle_{\mathcal{E}} \equiv \frac{1}{L_1L_2L_3L_4}\sum_n \langle U_4(n)\rangle_{\mathcal{E}}.$$

The LHS of this equation is a quantity that can easily be evaluated on the lattice (and does not require renormalization). Any deviation from the value on the RHS signals the dynamical breaking of center symmetry. We have thus shown that, within the particular gauge considered here, a local, gauge-dependent quantity, such as the link average, can be used as an order parameter for center symmetry.

We stress once more that the color diagonal structure of $\langle U_\mu(n)\rangle$ is in fact a consequence of the invariance under global color rotations (71) and applies to both the confined and the deconfined phases. Similarly, over a $\hat{C}$-invariant ensemble (see Sec. V C), we have

$$e^{i\pi\frac{\lambda_1}{2}}\langle U_4(n)\rangle^* e^{-i\pi\frac{\lambda_1}{2}} = \langle U_4(n)\rangle, \tag{81}$$

in both the confined and the deconfined phases. This implies

$$\langle U_4^{11}\rangle = \langle U_4^{22}\rangle^* \tag{82}$$

and

$$\langle U_4^{33}\rangle \in \mathbb{R}. \tag{83}$$

As a consequence, the determinant of $\langle U_4\rangle$ should always be real.

Similarly, for a $\tilde{g}\cdot\hat{C}\cdot\tilde{g}^\dagger$-invariant ensemble (see above), it can be shown that the charge conjugation constraints are

$$\langle U_4^{11}\rangle = e^{-i\frac{4\pi}{3L_4}}\langle U_4^{11}\rangle^* \tag{84}$$

and

$$\langle U_4^{22}\rangle = e^{i\frac{2\pi}{3L_4}}\langle U_4^{33}\rangle^*. \tag{85}$$

It follows that the first diagonal element lies in the direction of $e^{-i\frac{2\pi}{3L_4}}$, while the other two have the same modulus and their product has a phase fixed to $e^{i\frac{2\pi}{3L_4}}$. The product of the phases of the three diagonal elements is then real, ensuring once again that the determinant of $\langle U_4\rangle$ is real. Similar conclusions apply for a $\tilde{g}\cdot\hat{C}\cdot\tilde{g}^\dagger$-invariant ensemble, but this time the second diagonal element lies in the direction of $e^{i\frac{2\pi}{3L_4}}$, while the product of the other two has a phase fixed to $e^{-i\frac{2\pi}{3L_4}}$.

What center symmetry does is to further specify the relation between the various diagonal coefficients $\langle U_4^{ii}\rangle$ in the symmetric phase: up to a factor η, the diagonal elements are $e^{-i/L_4 2\pi/3}$, $e^{i/L_4 2\pi/3}$, and 1, and this for the three types of ensembles. Notice also that η being equal to $U_4^{\rho_3\rho_3}$, it needs to be real from Eq. (83), as announced above.

E. Results

Let us confront these theoretical expectations with lattice simulations for pure Yang-Mills theory.

The simulations reported here use the Wilson gauge action at $\beta = 6.0$, with gauge fixing relying on the functional (70) and using a Fourier accelerated steepest descent method as the optimization algorithm, with the help of Chroma [31] and PFFT [32] libraries. For this β value the simulations at zero temperature [33] suggest that finite lattice effects are small. The simulations consider two temperatures, one above T_c and another one below T_c for gauge-fixed ensembles with 100 gauge configurations. The lattice sizes used are $64^3\times 6$ and $64^3\times 8$. Measuring the temperature as $T = 1/aL_4$, with $1/a = 1.943$ GeV, the temperature for the $64^3\times 6$ lattice is $T = 324$ MeV, while the $64^3\times 8$ lattice corresponds to a $T = 243$ MeV. We recall that, in these units, for pure Yang-Mills theory, the temperature at which deconfinement occurs is ∼270 MeV. The starting configurations for the gauge-fixing algorithm are taken to be those in the Landau gauge which were already available from previous projects. Once a gauge-fixed ensemble is generated, we can generate two other ensembles in the same gauge by applying the transformations $\tilde{g}$ and $\tilde{g}^\dagger$. As explained above, in the low temperature phase, we expect these three ensembles to be essentially the same (see in particular Fig. 4 below), while in the high temperature phase, the three ensembles correspond to three different center sectors, characterized by different transformation properties under charge conjugation (see Sec. V C).

To illustrate the outcome of the simulations, we consider both the ensemble average link at a single lattice size, denoted as $\langle\cdots\rangle$, and its mean value over the lattice and gauge ensemble, denoted as $\langle\!\langle\cdots\rangle\!\rangle$. In what concerns the statistical errors, they were evaluated either by a single jackknife elimination or the bootstrap method with a 68% confidence level. When compared, both methods produce essentially the same estimations for the errors. The results for the average over lattice and gauge ensembles have smaller statistical errors. A full numerical account of these averages, including the statistical errors, is reported in Appendix C. Here we just show a simplified version of the results.

Let us start by the ensemble averages of the temporal link at a given lattice site. We shall take the origin of the lattice as an example, but we have checked that the observations to be made below apply to the other sites as well. For the temperature above the transition that uses the $64^3\times 6$ lattice it follows that, for each type of ensemble,

$$\langle U_4\rangle \approx 0.881\begin{pmatrix} 0.996\,e^{-0.140} & 0.030\,e^{i0.556} & 0.059\,e^{-i1.187}\\ 0.018\,e^{i1.648} & 0.995\,e^{i0.150} & 0.004\,e^{i1.833}\\ 0.055\,e^{-i2.170} & 0.007\,e^{i1.894} & 1.005\,e^{-i0.010}\end{pmatrix}, \tag{86}$$

$$\langle U_4^{\tilde{g}}\rangle \approx 0.881 \begin{pmatrix} 1.005\,e^{-i0.360} & 0.055\,e^{-i1.472} & 0.007\,e^{-i0.026} \\ 0.059\,e^{-i1.535} & 0.996\,e^{i0.558} & 0.030\,e^{-i1.364} \\ 0.004\,e^{i3.055} & 0.018\,e^{-i2.366} & 0.995\,e^{-i0.199} \end{pmatrix}, \tag{87}$$

$$\langle U_4^{\tilde{g}^\dagger}\rangle \approx 0.881 \begin{pmatrix} 0.995\,e^{-i0.548} & 0.004\,e^{-2.530} & 0.018\,e^{i1.997} \\ 0.007\,e^{-i0.375} & 1.005\,e^{i0.339} & 0.055\,e^{i2.892} \\ 0.030\,e^{-i0.142} & 0.059\,e^{i0.733} & 0.996\,e^{i0.209} \end{pmatrix}, \tag{88}$$

where the matrices have been obtained by factoring out the cubic root of the determinant of the link average. This determinant, which is of course the same for the three types of ensembles, is found to be $\det\langle U_4\rangle = (0.881)^3$. The matrices have a structure that is essentially diagonal, in agreement with color invariance constraints, and with the phases adding to zero, in agreement with charge conjugation invariance constraints. More precisely, we find that, for each ensemble, one of the diagonal elements is $\approx e^{i2\pi/3L_4 k} = e^{i0.349k}$ with $k = 0, -1$ or 1, while the product of the other two is $\approx e^{-i2\pi/3L_4 k} = e^{-i0.349k}$. As discussed above, center symmetry would require that the three diagonal elements are equal to $e^{i2\pi/3L_4 k}$, with $k = -1$, 1, and 0, no matter what type of ensemble is considered. Thus, the high temperature data indicate that center symmetry is broken.

On the other hand, with the low temperature data on the $64^3 \times 8$ lattice we find that

$$\langle U_4\rangle \approx 0.855 \begin{pmatrix} 0.995\,e^{-i0.230} & 0.068\,e^{i1.935} & 0.030\,e^{i2.597} \\ 0.053\,e^{i1.441} & 1.007\,e^{i0.284} & 0.026\,e^{-i1.429} \\ 0.040\,e^{i0.778} & 0.031\,e^{-i0.832} & 0.993\,e^{-i0.058} \end{pmatrix}, \tag{89}$$

$$\langle U_4^{\tilde{g}}\rangle \approx 0.855 \begin{pmatrix} 0.993\,e^{-i0.320} & 0.040\,e^{i1.302} & 0.031\,e^{-i2.665} \\ 0.030\,e^{i2.335} & 0.995\,e^{i0.294} & 0.068\,e^{i0.102} \\ 0.026\,e^{-i0.120} & 0.053\,e^{-i2.747} & 1.007\,e^{i0.022} \end{pmatrix}, \tag{90}$$

$$\langle U_4^{\tilde{g}^\dagger}\rangle \approx 0.855 \begin{pmatrix} 1.007\,e^{-i0.240} & 0.026\,e^{i0.404} & 0.053\,e^{i1.703} \\ 0.031\,e^{-i2.926} & 0.993\,e^{i0.203} & 0.040\,e^{-i0.531} \\ 0.068\,e^{i1.411} & 0.030\,e^{-i1.854} & 0.995\,e^{i0.032} \end{pmatrix}. \tag{91}$$

Although the results are not fully conclusive due to statistical errors, the data seem more compatible with an unbroken center symmetry where, no matter what ensemble is considered, the diagonal elements are close to $\approx e^{i2\pi/3L_4 k} = e^{i0.262k}$ with $k = -1$, 1, and 0.

To reduce the numerical errors, we now consider the double average, both over the ensemble and over the lattice sites. For a temperature above the transition, i.e., for the simulation using $L_4 = 6$, we find

$$\langle\langle U_4\rangle\rangle \approx 0.866 \begin{pmatrix} 1.000\,e^{-i0.169} & 0.000 & 0.000 \\ 0.000 & 1.000\,e^{i0.169} & 0.000 \\ 0.000 & 0.000 & 1.000\,e^{i0.000} \end{pmatrix}, \tag{92}$$

$$\langle\langle U_4^{\tilde{g}}\rangle\rangle \approx 0.866 \begin{pmatrix} 1.000\,e^{-i0.349} & 0.000 & 0.000 \\ 0.000 & 1.000\,e^{i0.529} & 0.000 \\ 0.000 & 0.000 & 1.000\,e^{-i0.180} \end{pmatrix}, \tag{93}$$

$$\langle\langle U_4^{\tilde{g}^\dagger}\rangle\rangle \approx 0.866 \begin{pmatrix} 1.000\,e^{-i0.529} & 0.000 & 0.000 \\ 0.000 & 1.000\,e^{i0.349} & 0.000 \\ 0.000 & 0.000 & 1.000\,e^{i0.180} \end{pmatrix}, \tag{94}$$

whereas, at a temperature below the transition corresponding to $L_4 = 8$, we find

$$\langle\langle U_4\rangle\rangle \approx 0.862 \begin{pmatrix} 1.000\,e^{-i0.257} & 0.000 & 0.000 \\ 0.000 & 1.000\,e^{i0.257} & 0.000 \\ 0.000 & 0.000 & 1.000\,e^{i0.000} \end{pmatrix}, \tag{95}$$

$$\langle\langle U_4^{\tilde{g}}\rangle\rangle \approx 0.862 \begin{pmatrix} 1.000\,e^{-i0.262} & 0.000 & 0.000 \\ 0.000 & 1.000\,e^{i0.267} & 0.000 \\ 0.000 & 0.000 & 1.000\,e^{-i0.005} \end{pmatrix}, \tag{96}$$

$$\langle\langle U_4^{\tilde{g}^\dagger}\rangle\rangle \approx 0.862 \begin{pmatrix} 1.000\,e^{-i0.266} & 0.000 & 0.000 \\ 0.000 & 1.000\,e^{i0.261} & 0.000 \\ 0.000 & 0.000 & 1.000\,e^{i0.005} \end{pmatrix}. \tag{97}$$

The main features described above on the case of the lattice origin are now more clearly visible. The matrices are clearly diagonal and follow the constraints of charge conjugation with the phases $e^{i0.349}$ and $e^{i0.262}$ playing a central role for the high and low temperature data, respectively. It is also now pretty clear that the low temperature data are compatible with an unbroken center symmetry, as the diagonal elements are all of the form $e^{i0.262k}$, thus reproducing the predicted structure given in Eq. (79). The high temperature data, in contrast, break the symmetry as two of the diagonal elements do not follow the

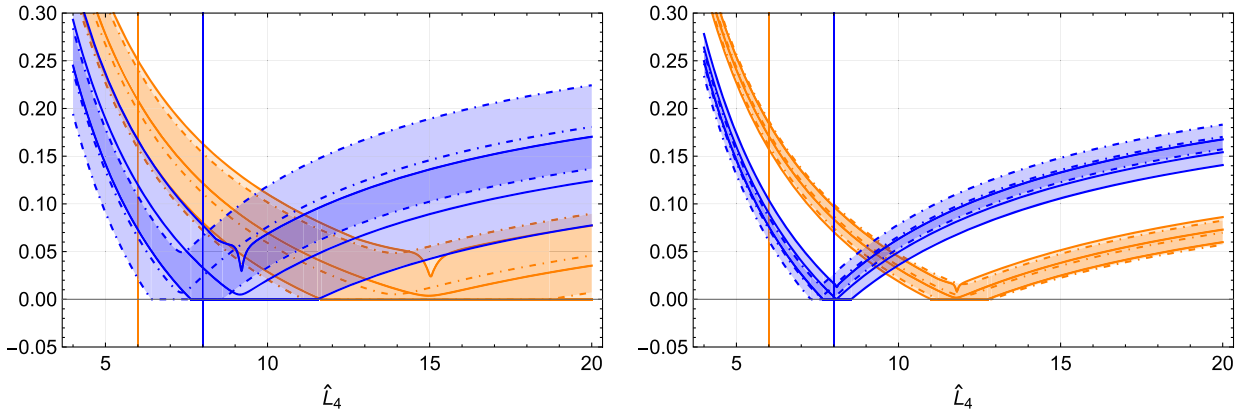


FIG. 1. Left plot: The distances $|M_{11} - \exp\{-i/\hat{L}_4 2\pi/3\}|$ and $|M_{22} - \exp\{i/\hat{L}_4 2\pi/3\}|$ at site $n = 0$ (plain and dash-dotted curves), as a function of an auxiliary parameter $\hat{L}_4$ that takes the value of the temporal lattice extent L_4 at the vertical line; see the main text for explanations. Low temperature data in blue ($L_4 = 8$) and high temperature data in orange ($L_4 = 6$). Right plot: the same for the average of $\langle U_4(n)\rangle/(\det\langle U_4(n)\rangle)^{1/3}$ over ten sites.

pattern $e^{i0.349k}$. Then, the numerical simulations confirm the theoretical predictions on the use of the average link as an order parameter for the transition from the confined to deconfined phase.

The particular role of the phases $\exp\{-i/L_4 2\pi/3\}$ and $\exp\{i/L_4 2\pi/3\}$ can be nicely illustrated by monitoring the distance (in the complex plane) between M_{11} (respectively, M_{22}), where $M \equiv \langle U_4\rangle/\eta$, and an arbitrary phase $\exp\{-i/\hat{L}_4 2\pi/3\}$ (respectively, $\exp\{i/\hat{L}_4 2\pi/3\}$) parametrized by a continuous external parameter $\hat{L}_4$ (see Fig. 1). The error bars result from the propagation of the error from the link average to the above-defined distances. At low temperature, we see that both distances are small (and essentially the smallest) when $\hat{L}_4$ takes the value of the

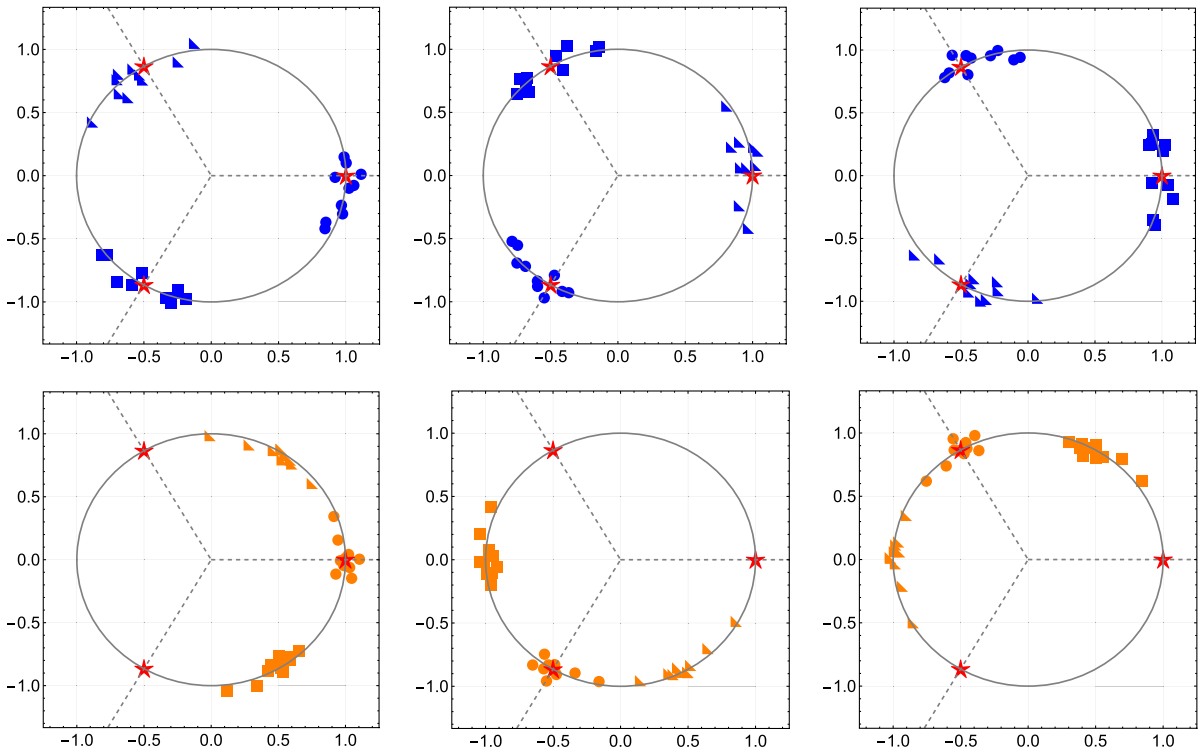


FIG. 2. Location in the complex plane of the first (squares), second (triangles), and third (circles) diagonal elements of M^{L_4} as obtained from averaging over gauge-fixed ensembles of the type 0 (left), + (middle), or − (right), below (top) and above (bottom) the deconfinement transition, at ten lattice sites.

lattice temporal extent L_4 (vertical blue line). This is not the case at high temperature. The left plot shows the analysis for the origin of the lattice but we have checked that the same pattern extends to the other sites of the lattice. In the right plot of Fig. 1, we show the corresponding test of (80) upon averaging over ten sites to reduce statistical fluctuations.

Finally, in Fig. 2, we show the location of the three diagonal elements of M, or more conveniently M^{L_4},[17] in the complex plane below and above the deconfinement transition, when averaging over three different gauge-fixed ensembles, $\mathcal{E}_{0\mathrm{gf}}$, $\mathcal{E}_{+\mathrm{gf}}$, and $\mathcal{E}_{-\mathrm{gf}}$ (see the discussion at the end of Sec. V C). In the confined phase, these three ensembles are essentially the same, and we see that the diagonal elements of M comply with the center symmetry constraints (80). In the deconfined phase, the constraints are violated in three different ways, depending on which ensemble is considered.

In line with the discussion above, we find that upon breaking the symmetry, one of the diagonal elements lies along $e^{ik2\pi/3}$, with $k = 0, -1$, or 1, while the product of the other two has a phase fixed to $e^{-ik2\pi/3}$.

Surprisingly, not only does one element remain along $e^{ik2\pi/3}$ but it is actually of modulus 1. We have found no explanation of this fact but, given this observation, we find that the matrix M is unitary. This is not obvious *a priori* since an average of unitary matrices such as $\langle U_\mu \rangle$ is not necessarily unitary. What we know from the very definition of M is that $\det M = 1$.

In the confined phase, the unitarity of M follows from the center-symmetry constraint (80). In the deconfined phase, we need to invoke color invariance which ensures that M is diagonal and charge conjugation which ensures that two of the diagonal elements have the same modulus ρ while their product has a phase that cancels that of the third element. Then, one can write $1 = \det M = \rho^2$, where we have used that the third element has modulus 1 as we have empirically observed in the data. It follows that $\rho = 1$ and thus that $|M_{11}| = |M_{22}| = |M_{33}| = 1$. This implies that M is unitary.

VI. ADDITIONAL REMARKS

A. Twisted links

To make the center symmetry constraints look simpler, in particular in view of a future discussion of general link correlators, it is useful to work in terms of twisted link variables.

First, it is convenient to rewrite the explicit diagonal matrix in Eq. (70) as

$$e^{i\frac{\hat{\mu}_4}{L_4}\frac{4\pi}{3}\frac{\lambda_3}{2}} = g_c^\dagger(n+\hat{\mu})g_c(n), \tag{98}$$

with

$$g_c(n) \equiv e^{-i\frac{n_4}{L_4}\frac{4\pi}{3}\frac{\lambda_3}{2}}. \tag{99}$$

Then, the functional in (70) is rewritten as

$$\begin{aligned}\tilde{F}[U] &= \sum_{n,\mu} \mathrm{Re\ tr}\, g_c^\dagger(n+\hat{\mu})g_c(n)U_\mu(n) \\ &= \sum_{n,\mu} \mathrm{Re\ tr}\, g_c(n)U_\mu(n)g_c^\dagger(n+\hat{\mu}) \\ &= \sum_{n,\mu} \mathrm{Re\ tr}\, U_\mu^{g_c}(n),\end{aligned} \tag{100}$$

which looks like the standard Landau gauge functional, but for the transformed link variable $U_\mu^{g_c}$, which we refer to as a twisted link in what follows. Note that $g_c(n)$ is not periodic, not even periodic modulo a center element, so the twisted links are not periodic along the temporal directions. But one can construct correlators of twisted links from which it is very simple to retrieve (if needed) the correlators of the original links.

Now, since

$$(U_\mu^{g_0})^{g_c} = U_\mu^{g_c g_0} = U_\mu^{g_c g_0 g_c^\dagger g_c} = (U_\mu^{g_c})^{g_c g_0 g_c^\dagger}, \tag{101}$$

the maximization of the functional $\tilde{F}[U]$ over the $\mathcal{G}_0$-orbit of U_μ is equivalent to the maximization of the standard Landau gauge functional $\sum_{n,\mu} \mathrm{Re\,tr} U_\mu(n)$ over the $g_c\mathcal{G}_0 g_c^\dagger$-orbit of $U_\mu^{g_c}$. The elements of this orbit are all twisted links, that is, of the form $U_\mu^{g_c}$ with U_μ periodic. It follows that the gauge fixing associated with the gauge $\tilde{F}[U]$ can be interpreted as a gauge fixing associated with the standard Landau gauge, to the price of working with twisted links (obeying modified, nonperiodic, boundary conditions) and to replacing $\mathcal{G}_0$ by $g_c\mathcal{G}_0 g_c^\dagger$ which is different from $\mathcal{G}_0$.

An interesting property of the twisted links is that they transform in a simpler way than the standard links. Indeed, under a center transformation (12), one has

$$\begin{aligned}U_\mu^{g_c}(n) \to\ & g_c(n)\tilde{g}(n)g_c^\dagger(n)U_\mu^{g_c}(n) \\ & \times g_c(n+\hat{\mu})\tilde{g}^\dagger(n+\hat{\mu})g_c^\dagger(n+\hat{\mu}).\end{aligned} \tag{102}$$

But from Eqs. (98) and (61), we have

$$\begin{aligned}& g_c(n+\hat{\mu})\,\tilde{g}^\dagger(n+\hat{\mu})\,g_c^\dagger(n+\hat{\mu}) \\ &= g_c(n)e^{-i\frac{\hat{\mu}_4}{L_4}\frac{4\pi}{3}\frac{\lambda_3}{2}}\tilde{g}^\dagger(n+\hat{\mu})g_c^\dagger(n+\hat{\mu}) \\ &= g_c(n)\tilde{g}^\dagger(n)e^{-i\frac{\hat{\mu}_4}{L_4}\frac{4\pi}{3}\frac{\lambda_3}{2}}g_c^\dagger(n+\hat{\mu}) \\ &= g_c(n)\tilde{g}^\dagger(n)g_c^\dagger(n) = (g_c(n)\tilde{g}(n)g_c^\dagger(n))^\dagger.\end{aligned} \tag{103}$$

[17] In particular, note that the center symmetry constraint on M^{L_4} is the one that remains nontrivial in the continuum limit (corresponding to $L_4 \to \infty$ at fixed temperature).

In other words, at each lattice site n, the twisted link transforms under a local color rotation. For later use, let us also mention that, in terms of twisted links, charge conjugation reads

$$U_\mu^{g_c}(n) \to g_c(n)e^{i\pi\frac{\lambda_1}{2}}g_c(n)(U_\mu^{g_c})^*(n)g_c^\dagger(n+\hat{\mu})e^{-i\pi\frac{\lambda_1}{2}} \times g_c^\dagger(n+\hat{\mu}). \tag{104}$$

Using

$$g_c(n)e^{i\pi\frac{\lambda_1}{2}}g_c(n) = e^{i\pi\frac{\lambda_1}{2}}, \tag{105}$$

this becomes

$$U_\mu^{g_c}(n) \to e^{i\pi\frac{\lambda_1}{2}}(U_\mu^{g_c}(n))^* e^{-i\pi\frac{\lambda_1}{2}}, \tag{106}$$

with the same consequences as (72).

Denoting the twisted links by $\hat{U}_\mu(n)$ and

$$\hat{g}(n) \equiv g_c(n)\tilde{g}(n)g_c^\dagger(n), \tag{107}$$

we have this time

$$\langle\hat{U}_\mu(n)\rangle = \hat{g}(n)\langle\hat{U}_\mu(n)\rangle\hat{g}^\dagger(n). \tag{108}$$

To deduce the constraints on $\langle\hat{U}_\mu(n)\rangle$ which is again diagonal due to color invariance, we can first investigate the adjoint action of $\hat{g}(n)$ on a diagonal matrix X. This is actually quite simple because the same n appears on the left and on the right of the transformation. Then all the factors contributing to $\hat{g}(n)$ that correspond to phase multiplications of the diagonal elements do not play any role, and we are left only with the color rotations included in $\tilde{g}(n)$. Those correspond to the permutation $X_{11} \leftrightarrow X_{22}$, followed by $X_{11} \leftrightarrow X_{33}$. This gives

$$\hat{g}(n)\begin{pmatrix} X_{11} & 0 & 0 \\ 0 & X_{22} & 0 \\ 0 & 0 & X_{33} \end{pmatrix}\hat{g}^\dagger(n) = \begin{pmatrix} X_{33} & 0 & 0 \\ 0 & X_{11} & 0 \\ 0 & 0 & X_{22} \end{pmatrix}, \tag{109}$$

corresponding to the cyclic permutation

$$(X_{11}, X_{22}, X_{33}) \to (X_{33}, X_{11}, X_{22}). \tag{110}$$

It follows that the constraint (108) is rewritten as

$$\langle\hat{U}_\mu^{11}(n)\rangle = \langle\hat{U}_\mu^{22}(n)\rangle = \langle\hat{U}_\mu^{33}(n)\rangle \tag{111}$$

and implies

$$\langle\hat{U}_\mu(n)\rangle = \eta\mathbb{1}. \tag{112}$$

Of course, this can also be directly deduced from (78).

It is finally interesting to switch to another basis. Indeed, any diagonal complex matrix writes as

$$X = X_1\mathbb{1} + X_3\frac{\lambda_3}{2} + X_8\frac{\lambda_8}{2}, \tag{113}$$

with

$$X_1 = \frac{1}{3}\mathrm{tr}X = \frac{X_{11}+X_{22}+X_{33}}{3}, \tag{114}$$

$$X_3 = \mathrm{tr}[X\lambda_3] = X_{11} - X_{22}, \tag{115}$$

$$X_8 = \mathrm{tr}[X\lambda_8] = \frac{X_{11}+X_{22}-2X_{33}}{\sqrt{3}}. \tag{116}$$

Under the cyclic permutation (110), the components in the new basis transform as

$$X_1 \to X_1, \tag{117}$$

$$X_3 \to X_{33} - X_{11} = -\frac{1}{2}X_3 - \frac{\sqrt{3}}{2}X_8, \tag{118}$$

$$X_8 \to \frac{X_{33}+X_{11}-2X_{22}}{\sqrt{3}} = -\frac{1}{2}X_8 + \frac{\sqrt{3}}{2}X_3, \tag{119}$$

so the first component does not change while the vector (X_3, X_8) rotates by an angle $2\pi/3$.

This means that the constraint (108) implies that the vector $(\langle\hat{U}_\mu^3(n)\rangle, \langle\hat{U}_\mu^8(n)\rangle)$ is invariant under this rotation, and thus that

$$\langle\hat{U}_\mu^3(n)\rangle = \langle\hat{U}_\mu^8(n)\rangle = 0, \tag{120}$$

if center symmetry is not broken. We also note that, for a $\hat{C}$-invariant ensemble, Eqs. (82) and (83) combined with Eqs. (115) and (116) imply that $\langle\hat{U}_\mu^8(n)\rangle$ is real while $\langle\hat{U}_\mu^3(n)\rangle$ is imaginary.[18] So, the breaking of center symmetry should be visible by monitoring $\mathrm{Im}\langle\hat{U}_\mu^3(n)\rangle$ or $\mathrm{Re}\langle\hat{U}_\mu^8(n)\rangle$.

In Fig. 3, we evaluate the vectors $(\mathrm{Re}\hat{U}_4^3, \mathrm{Re}\hat{U}_4^8)$ and $(\mathrm{Im}\,\hat{U}_4^3, \mathrm{Im}\,\hat{U}_4^8)$ at site $n = 0$ for all the configurations of our $\hat{C}$-invariant ensembles $\mathcal{E}_{0\mathrm{gf}}$ below and above the transition temperature.[19] We see that, below the transition, all these quantities fluctuate around 0 within errors, in agreement with the center symmetry constraints. Above the

[18]For the other possible ensembles, the constraints are different. In particular, one finds that $\mathrm{Im}\langle\hat{U}_\mu^8(n)\rangle = \pm\sqrt{3}\,\mathrm{Im}\langle\hat{U}_\mu^3(n)\rangle$, in line with Fig. 4.

[19]We show the real part (respectively, the imaginary parts) together on the same plot because these are the components that are related to each other by the center symmetry, according to Eqs. (118) and (119).

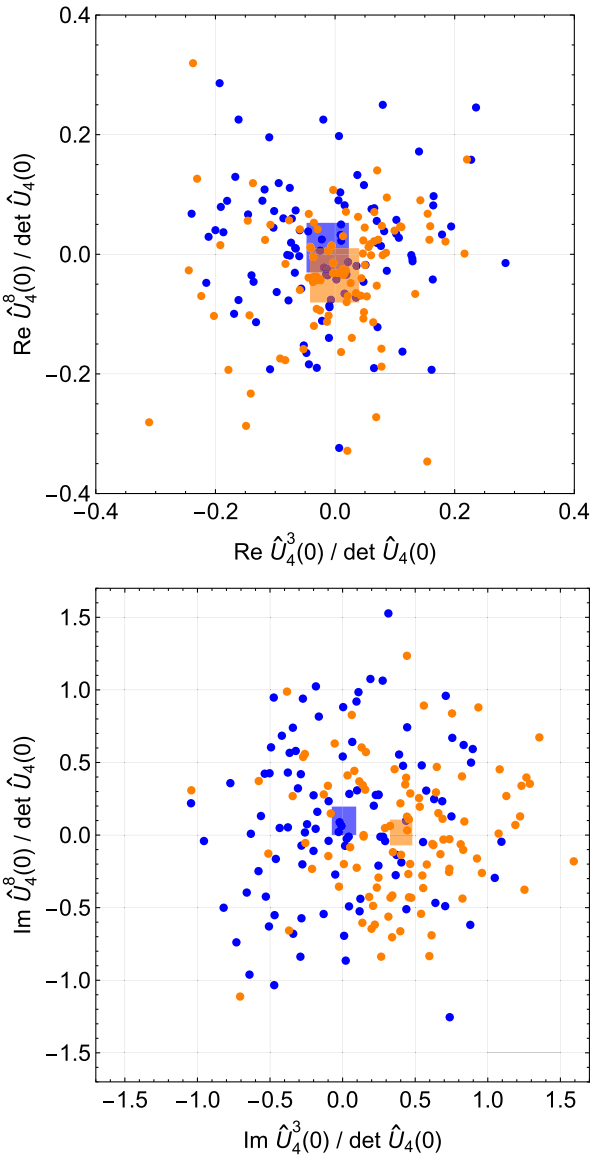


FIG. 3. Spread of the real and imaginary parts of $\hat{U}_4^3(n=0)/\det\hat{U}_4(n=0)$ and $\hat{U}_4^8(n=0)/\det\hat{U}_4(n=0)$ below (blue) and above (orange) the transition temperature. The respective mean values and standard deviations are represented by the shaded rectangles.

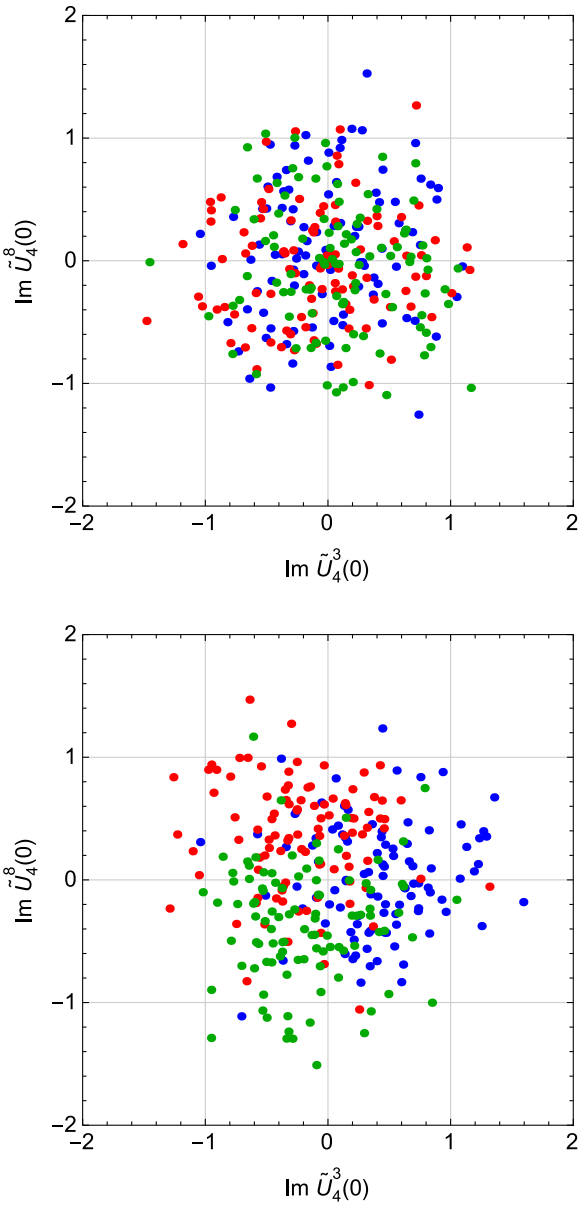


FIG. 4. The three gauge-fixed ensembles $\mathcal{E}_{0,\mathrm{gf}}$ (blue), $\mathcal{E}_{-,\mathrm{gf}} = \mathcal{E}_{0,\mathrm{gf}}^{g}$ (red), and $\mathcal{E}_{+,\mathrm{gf}} = \mathcal{E}_{0,\mathrm{gf}}^{g^\dagger}$ (green), projected along $\mathrm{Im}\,\hat{U}_4^3(0)$ and $\mathrm{Im}\,\hat{U}_4^8(0)$, together with their transformation under g and $g^\dagger$. Top: below the transition. Bottom: above the transition.

transition, one of these quantities, $\mathrm{Im}\,\hat{U}_4^3(n=0)$, starts developing fluctuations around a nonzero value, signaling the breaking of center symmetry. We find that $\mathrm{Re}\hat{U}_4^8(n=0)$ seems to keep fluctuating around 0, but it could be that it fluctuates around a value which is negligible with respect to the mean value of $\mathrm{Im}\,\hat{U}_4^3(n=0)$.

This order parameter pattern can be nicely visualized by looking at the link averages over the three possible ensembles $\mathcal{E}_{0,\mathrm{gf}}$, $\mathcal{E}_{-,\mathrm{gf}} = \mathcal{E}_{0,\mathrm{gf}}^{\tilde{g}}$, and $\mathcal{E}_{+,\mathrm{gf}} = \mathcal{E}_{0,\mathrm{gf}}^{\tilde{g}^\dagger}$ (see Fig. 4). In the symmetric phase, the system explores enough phase space, and the three ensembles are essentially the same (see the top plot of Fig. 4).

In the broken phase, the system gets stuck in a given sector characterized by the value of the vector $(\mathrm{Im}\langle U_4^3\rangle, \mathrm{Im}\langle U_4^8\rangle)$[20] (see the bottom plot of Fig. 4).

[20]It may seem strange that $\mathrm{Im}\langle U_4^8\rangle$ takes a nonzero value since we said above that $\langle U_4^8\rangle$ should be real from charge conjugation invariance. However, as we already pointed out, in the broken phase, this statement applies only to the average over the $\hat{C}$-invariant ensemble.

B. Mapping the gluon field

So far, we have considered link averages. However, in the continuum theory, we work with gauge fields. It is thus interesting to look at the gauge field average. A nontrivial check is whether one retrieves the center symmetry constraint for the gluon field average

$$\beta_T \langle A_4^3(x)\rangle = -\frac{4\pi}{3} \tag{121}$$

with $\beta_T \equiv 1/T$, that is, expected in the continuum (see the Appendix A).

The links are path ordered exponentiations of the gluon fields and, for sufficiently small lattice spacing, one can write

$$U_4(n) = e^{iaA_4(x)}, \tag{122}$$

where $A_4(x) \equiv A_4^a(x)t^a$ and x is a point between na and $(n+\hat{4})a$, where $\hat{4}$ is the unit vector along Euclidean time direction and a is the lattice spacing, for instance, $x = (n+\hat{4}/2)a$. As usual, the exponential is defined via its Taylor series, that is, an expansion in aA and, typically, the terms are labeled by the corresponding power of the lattice spacing.

Let us first consider this expansion to linear order in aA:

$$U_4(n) = \mathbb{1} + iaA_4(x) + \mathcal{O}(a^2). \tag{123}$$

Upon taking the dagger of this expression, one finds

$$U_4^\dagger(n) = \mathbb{1} - iaA_4(x) + \mathcal{O}(a^2), \tag{124}$$

and because the $\mathcal{O}(a^2)$ terms are Hermitian, one gets

$$U_4(n) - U_4^\dagger(n) = 2iaA_4(x) + \mathcal{O}(a^3). \tag{125}$$

This means that the quantity

$$aA_4^{\mathrm{LO}}(x) \equiv \frac{U_4(n) - U_4^\dagger(n)}{2i} \tag{126}$$

provides an estimate of aA to a^3 accuracy:

$$aA_4^{\mathrm{LO}}(x) = aA_4(x) + \mathcal{O}(a^3), \tag{127}$$

from which one can evaluate the average of aA to a^3 accuracy:

$$\langle aA_4^{\mathrm{LO}}(x)\rangle = \langle aA_4(x)\rangle + \mathcal{O}(a^3). \tag{128}$$

and also the double average. For the latter, using this estimate on our low temperature data, we find[21]

$$\beta_T \langle\langle A_4^{\mathrm{LO},3}\rangle\rangle = -3.5079(60), \tag{129}$$

which is not exactly close to the expected value $-4\pi/3 \simeq -4.18879$.

One possible culprit is that aA might not be small enough for the higher order terms in Eq. (123) to be negligible. One simple way to illustrate this is to notice that Eq. (123) implies

$$\det\langle U_4(n)\rangle = 1 + \mathcal{O}(a^2), \tag{130}$$

where we used that $\det(\mathbb{1} + \delta M) \simeq 1 + \mathrm{tr}\delta M$ as well as $\mathrm{tr}t^a = 0$. Therefore, even though the average of a link is not a unitary matrix, its determinant should approach 1 in the continuum limit, at least according to (123). Our results in the previous section show, however, that $\det\langle U_4(n)\rangle$ deviates from 1 by 36% in both the confined and deconfined phases. This indeed indicates that higher order terms in Eq. (123) should be considered. And, in fact, the next-to-leading term in (131) can be expressed in terms of the connected two-point correlator

$$\det\langle U_4(n)\rangle = 1 - \frac{a^2}{2}\mathrm{tr}\langle (A - \langle A\rangle)^2\rangle + \mathcal{O}(a^4), \tag{131}$$

and represents a negative contribution. It would be interesting to evaluate this contribution and compare it to the observed deviation, but we leave it for a future investigation where we will have a closer look at the propagator.

We have considered higher order terms that correct Eq. (125) and thus our determination of the gluon field from the links. Let us illustrate how this works to obtain a determination of aA from the links valid to a^5 accuracy. The trick is to write Eq. (125) to next order:

$$U_4(n) - U_4^\dagger(n) = 2iaA_4(x) - \frac{1}{3}i(aA_4(x))^3 + \mathcal{O}(a^5), \tag{132}$$

and a similar expansion for $U_4^2 - (U_4^\dagger)^2$

$$(U_4(n))^2 - (U_4^\dagger(n))^2 = 4iaA_4(x) - \frac{8}{3}i(aA_4(x))^3 + \mathcal{O}(a^5), \tag{133}$$

and to find a linear combination of the two that kills the terms of order a^3. This linear combination is easily found to be

$$\begin{aligned} &8(U_4(n) - U_4^\dagger(n)) - ((U_4(n))^2 - (U_4^\dagger(n))^2) \\ &= 12iaA_4(x) + \mathcal{O}(a^5). \end{aligned} \tag{134}$$

It follows that

[21] Statistical errors computed with the jackknife method.

$$aA_4^{\mathrm{NLO}}(x) \equiv \frac{2}{3}\frac{U_4(n)-U_4^\dagger(n)}{i} - \frac{1}{12}\frac{((U_4(n))^2-(U_4^\dagger(n))^2}{i} \quad (135)$$

provides an estimate of aA to a^5 accuracy:

$$aA_4^{\mathrm{NLO}}(x) = aA_4(x) + \mathcal{O}(a^5), \quad (136)$$

from which one can evaluate the average of aA to a^5 accuracy:

$$\langle aA_4^{\mathrm{NLO}}(x)\rangle = \langle aA_4(x)\rangle + \mathcal{O}(a^5). \quad (137)$$

Similarly, one can construct an estimator of aA to a^7 accuracy that also involves U_4^3

$$aA_4^{\mathrm{NNLO}}(x) \equiv \frac{3}{4}\frac{U_4(n)-U_4^\dagger(n)}{i} - \frac{3}{20}\frac{((U_4(n))^2-(U_4^\dagger(n))^2}{i} + \frac{1}{60}\frac{((U_4(n))^3-(U_4^\dagger(n))^3}{i}. \quad (138)$$

Using these estimators on our low temperature data, we find

$$\beta_T\langle\!\langle A_4^{\mathrm{NLO},3}\rangle\!\rangle = -3.8291(67) \quad (139)$$

and

$$\beta_T\langle\!\langle A_4^{\mathrm{NNLO},3}\rangle\!\rangle = -3.8741(68), \quad (140)$$

respectively, which improve over the leading order estimate (129) and seem to approach the expected continuum value.

Let us mention that the deviation (129) that we observed at leading order could have been anticipated using the center symmetry constraints on the link average and the measured value of $\eta \neq 1$. Indeed, one can plug (79) in the RHS of Eq. (126), multiply by L_4, and use $aL_4 = \beta_T$ to arrive at

$$\beta_T\langle\!\langle A_4^{\mathrm{LO},3}\rangle\!\rangle = -\eta\frac{4\pi}{3}. \quad (141)$$

With the value of $\eta \simeq 0.862$ found in the previous section, we arrive at

$$\beta_T\langle\!\langle A_4^{\mathrm{LO},3}\rangle\!\rangle \simeq -3.61, \quad (142)$$

not far from the leading order result (129) quoted above. It would be interesting to repeat the same exercise for the improved formulas relating the link to the gauge field and see if one gets indeed a result closer to $-4\pi/3$ as obtained in Eqs. (139) and (140).[22] Also, it would be interesting to compute the gluon field from the twisted links, since in that case we have $\beta_T\langle\tilde{A}_4^3(x)\rangle = 0$. Furthermore, one also needs to study the continuum limit by performing simulations with smaller lattice spacings. Finally, another possibility is that the relation (122) needs to be revisited.[23] We leave these interesting questions for future work.

Our study shows that higher terms in the relation between the link and the gluon field have a sizable effect on the outcome and should not be ignored. In general, the inclusion of the higher order terms is not a trivial exercise. A particular example is the evaluation of the plaquette in lattice perturbation theory in comparison to the outcome of Monte Carlo simulations that shows a sizable difference, oftentimes interpreted as originating from a nonperturbative contribution that is associated with the gluon condensate $\langle G^2\rangle$ (see, e.g., [34–36] and reference therein).

C. Gribov copies

In this section, we study the transformation properties of our center-symmetric Landau gauge-fixed ensemble under $\tilde{g}$. The diagonal components of the links transform according to Eq. (63). This means that to test whether the center-symmetry Landau gauge-fixed ensemble is approximately invariant under $\tilde{g}$, we can compare $U_4^{11}(n)$ and $e^{-\frac{i}{L_4}\frac{4\pi}{3}}U_4^{22}(n)$ on the available configurations. This comparison is shown in the upper plots of Fig. 5, together with a similar comparison for the Landau gauge configurations in the lower plots, in which case we do not expect the gauge-fixed ensemble to be invariant under $\tilde{g}^\dagger$. One clearly sees a difference between the configurations in those two gauges. In the former case, the sets $U_4^{11}(n)$ and $e^{-\frac{i}{L_4}\frac{4\pi}{3}}U_4^{22}(n)$ are quite different from each other, both at low and at high temperatures. In the case of the center-symmetric Landau gauge in contrast, the sets look pretty much on top of each

[22] This would require deriving the symmetry constraints for objects such as $\langle U^2\rangle$ or $\langle U^3\rangle$.

[23] Before gauge fixing, the functional integral is dominated by pure gauge configurations of the form $g_0(n)g_0^\dagger(n+\hat{\mu})$, where $g_0(n)$ is arbitrary and has no reason to become smooth in the continuum. Close to the continuum limit, the links that dominate are then of the form $U_\mu(n) = g_0(n)e^{iaA_\mu^a(x+(a/2)\hat{\mu})t^a}g_0^\dagger(n+\hat{\mu})$ but because $g_0(n)$ is not necessarily smooth, some of these links do not approach 1 in the continuum. As long as one remains at a non-gauge-fixed level and evaluates observables such that $\mathcal{O}[U^{g_0}] = \mathcal{O}[U]$, this is not a problem because the observables do not see the gauge transformation $g_0(n)$ and one can do as if all links that dominate where of the form (123). In contrast, within a generic gauge-fixed setting, the configurations of the gauge-fixed ensemble remain *a priori* of the general form above, unless the considered gauge and the selection of copies lead to smooth enough g_0's. It would require a separate study, far beyond the scope of the present one, to analyze whether this actually happens in the Landau gauge or in the present center-symmetric Landau gauge.

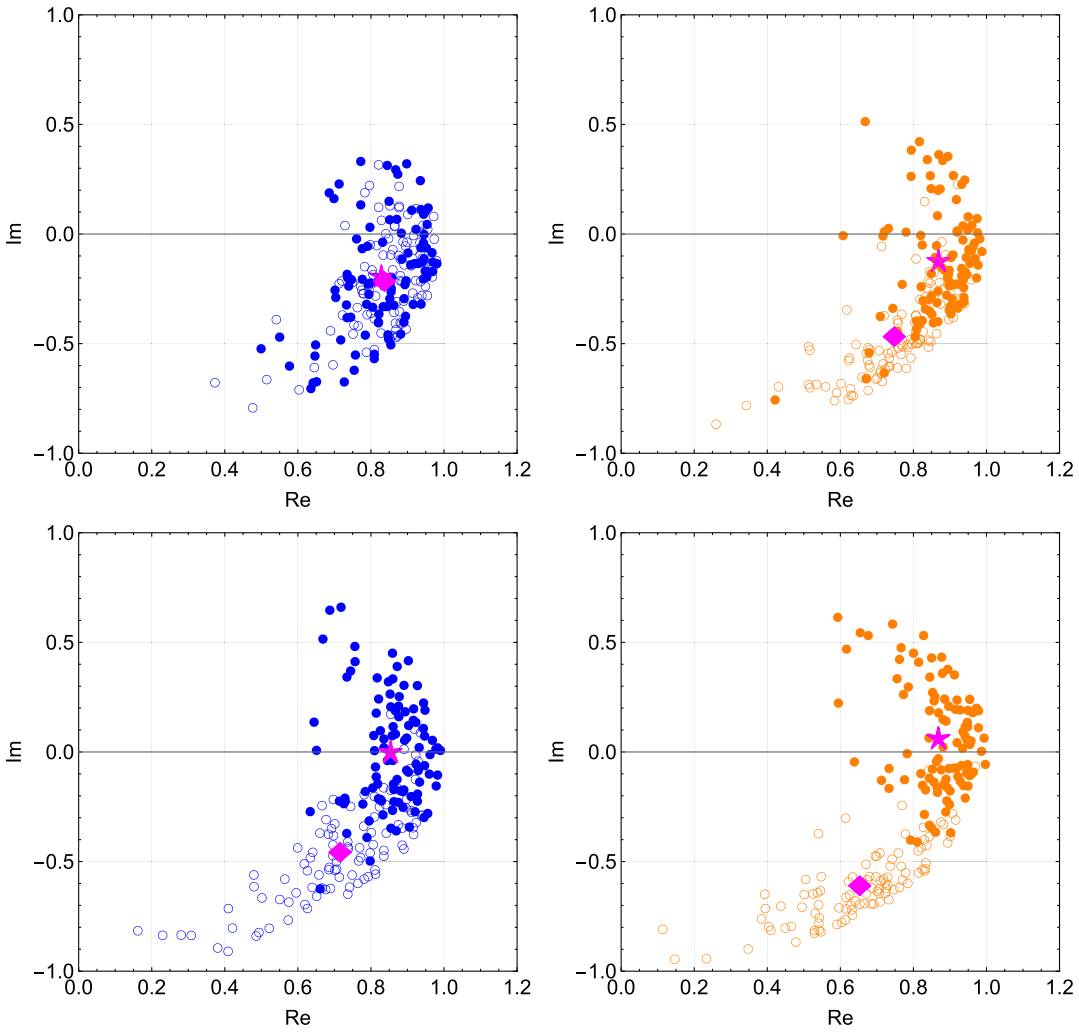


FIG. 5. The real and imaginary parts of the configurations $U_4^{11}(0)$ (plain circles) and $e^{-\frac{i}{L_4}\frac{4\pi}{3}}U_4^{22}(0)$ (empty circles), at low (blue, left) and high (orange, right) temperatures. The purple stars and purple diamonds represent the corresponding configuration averages. Top plot: center-symmetric Landau gauge configurations. Bottom plot: Landau gauge configurations.

other at low temperatures, and start deviating slightly only at high temperatures.

The same results can be illustrated by computing the distance[24] between the sets $U_4^{11}(n)$ and $e^{-\frac{i}{\hat{L}_4}\frac{4\pi}{3}}U_4^{22}(n)$ with $\hat{L}_4$ some auxiliary variable, both in the center-symmetric Landau gauge and in the standard Landau gauge (see Fig. 6). One clearly sees that nothing peculiar happens in the Landau gauge when $\hat{L}_4$ becomes equal to the lattice temporal extent L_4. In contrast, in the center-symmetric Landau gauge, the distance between the two sets is minimized at low temperatures around $\hat{L}_4 = 8$, the appropriate lattice value for the low temperature data. In the case of the high temperature data, the distance is minimized for a value of $\hat{L}_4$, that has nothing to do with the lattice value $\hat{L}_4 = 6$.

These results illustrate that despite the presence of Gribov copies, our gauge-fixing procedure produces an approximately $\tilde{g}$-invariant ensemble in the symmetric phase. Note also that our center-symmetric Landau gauge-fixed ensemble was produced by starting from an already available Landau gauge-fixed ensemble. That the final gauge-fixed ensemble turns out to be approximately $\tilde{g}$-invariant seems to be in line with the discussion at the end of Sec. IV E.

VII. CONCLUSIONS

In this work, we have considered the lattice implementation of gauge-fixed pure Yang-Mills theories at finite temperature and discussed under which conditions the link

[24]Given two sets Z_1 and Z_2 of N points each in the complex, we define their relative distance as

$$\frac{1}{N}\sum_{z_1\in Z_1}\mathrm{Min}_{z_2\in Z_2}|z_1 - z_2|.$$

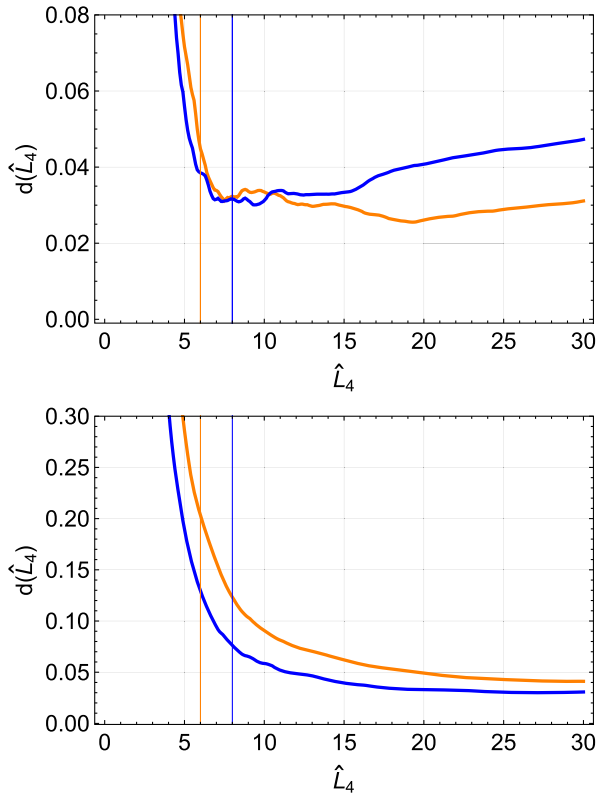


FIG. 6. The distance between the sets $U_4^{11}(0)$ and $e^{-\frac{i}{\hat{L}_4}\frac{4\pi}{3}}U_4^{22}(0)$ as a function of the control parameter $\hat{L}_4$, at low (blue) and high (orange) temperatures. Top plot: center-symmetric Landau gauge; Bottom plot: Landau gauge. The vertical lines represent the lattice values of the parameter $\hat{L}_4$ (8 at low temperature and 6 at high temperature).

correlators evaluated in a given gauge could be used as order parameters for center symmetry. This analysis singles out certain gauges which we refer to as center symmetric.

We have then implemented one particular example of a center-symmetric gauge, which corresponds in the continuum to the center-symmetric Landau gauge of Ref. [16]. Focusing on the link average, we have identified and solved the center symmetry constraints for this quantity. We have then tested these formal expectations on actual lattice data at temperatures below and above the transition. In the low temperature simulations, we find that the numerical link average accurately fulfills the center symmetry constraints, while the constraints are violated in the high temperature data. These numerical results show very clearly that the link average plays indeed the role of an order parameter for center symmetry in that gauge. This result provides alternative ways to explore the confinement/deconfinement transition beyond the usual program based on the Polyakov loop. In frameworks, such as continuum calculations, where the Polyakov loop is not so easily accessed, this is certainly a valuable piece of information.

On the lattice side, beyond increasing the statistics and the number of accessible temperature values, a natural continuation of this work is of course the evaluation of the two-link correlator and the associated gluon propagator which has been shown to behave as an order parameter in this gauge as well, at least within the Curci-Ferrari setup (see Ref. [17]). The same goes for the ghost propagator. It would also be interesting to extend the analysis to the SU(2) case where the transition is second order. In this case, we expect, if not a divergence, a large enhancement of the zero-momentum propagator at the transition, along the lines of what is observed in Ref. [18].

Other possible directions include the study of higher-order link correlators for which there are also symmetry constraints [17], as well as the inclusion of dynamical quarks. In this latter case, center symmetry is broken explicitly by the quark boundary conditions and the transition becomes a crossover for small enough quark masses. Still, we expect the link average to grant access to the crossover temperature.

ACKNOWLEDGMENTS

This work was supported by FCT—Fundação para a Ciência e a Tecnologia, I. P., under Projects No. UIDB/04564/2020 [37], No. UIDP/04564/2020 [38], and No. CERN/FIS-PAR/0023/2021 [39]. P. J. S. acknowledges financial support from FCT Contract No. CEECIND/00488/2017 [40]. The authors acknowledge the Laboratory for Advanced Computing at the University of Coimbra ([41]) and the Minho Advanced Computing Center ([42]) for providing access to the HPC resources. Access to Navigator was partly supported by the FCT Advanced Computing Projects No. 2021.09759.CPCA [43], No. 2022.15892.CPCA.A2 and No. 2023.10947.CPCA.A2. Access to Deucalion was supported by the FCT Advanced Computing Project No. 2024.11063.CPCA.A3. P. J. S. thanks CNRS for the financial support and CPHT, École Polytechnique, for the hospitality, where part of this work was performed.

DATA AVAILABILITY

The data that support the findings of this article are not publicly available upon publication because it is not technically feasible and/or the cost of preparing, depositing, and hosting the data would be prohibitive within the terms of this research project. The data are available from the authors upon reasonable request.

APPENDIX A: FROM THE DISCRETE TO THE CONTINUUM CENTER-SYMMETRIC LANDAU GAUGE

We claimed in the main text that the lattice gauge fixing based on the functional (70) corresponds to the center-symmetric Landau gauge in the continuum [16]. Let us here discuss how this comes about.

In fact, we shall more generally show that the discrete gauge fixing based on the functional

$$F_{\bar{A}}[U] \equiv \sum_{n,\mu} \mathrm{Re\,tr}[e^{-ia\bar{A}\hat{\mu}_4} U_\mu(n)], \tag{A1}$$

with $\bar{A} \equiv \bar{A}^j t^j$ constant, $t^j = \lambda_j/2$ the diagonal Gell-Mann matrices, and $a = \beta/L_4$ the lattice spacing, is the discrete version of the continuum gauge fixing

$$\partial_\mu (A^a_\mu - \bar{A}^a_\mu) - f^{abc} \bar{A}^b_\mu (A^c_\mu - \bar{A}^c_\mu) = 0, \tag{A2}$$

in the presence of a constant, temporal, and diagonal background $\bar{A}^a_\mu(x) = \delta_{\mu 4} \bar{A}^j \delta^{aj}$ and where f^{abc} denotes the SU(3) structure constants. These gauges are particular instances of continuum background Landau gauges. More generally, $\bar{A}^a_\mu$ could be an arbitrary configuration, and we stress that the gauge-fixing condition transforms covariantly under the simultaneous gauge transformation of the background field and the fluctuating field:

$$(\bar{A}^g_\mu)^a(x) \equiv (g(x)\bar{A}_\mu(x)g^\dagger(x))^a - ig(x)\partial_\mu g^\dagger(x), \tag{A3}$$

$$(A^g_\mu)^a(x) \equiv (g(x)A_\mu(x)g^\dagger(x))^a - ig(x)\partial_\mu g^\dagger(x). \tag{A4}$$

In what follows, however, we stick to backgrounds of the form $\bar{A}^a_\mu(x) = \delta_{\mu 4}\bar{A}^j\delta^{aj}$.

Note that, to comply with the lattice conventions used in the main text, we choose different sign conventions for covariant derivatives and gauge transformations in the continuum from the ones used in Ref. [16]. One can simply connect with the conventions in that reference upon making the changes $A \to -A$ and $\bar{A} \to -\bar{A}$. Accordingly also, what we have here defined as the Polyakov loop would correspond to the anti-Polyakov loop in that reference.

To connect with the continuum, we shall first make explicit the condition for a link configuration $U_\mu(n)$ to be a local maximum (and, more generally, an extremum) of the functional (A1) along the corresponding $\mathcal{G}_0$-orbit. In a second step, we will make use of the explicit relation between the link variables and the continuum gauge field:

$$U_\mu(n) - U^\dagger_\mu(n) = 2iaA^a_\mu(x)t^a + \mathcal{O}(a^3), \tag{A5}$$

where we take $x = (n + \hat{\mu}/2)a$. This is rewritten as

$$\mathbb{A}^a_\mu(n) = A^a_\mu(x) + \mathcal{O}(a^2), \tag{A6}$$

where we have introduced

$$\mathbb{A}^a_\mu(n) \equiv \frac{2}{a}\mathrm{Im\ tr}[t^a U_\mu(n)], \tag{A7}$$

for later convenience. It should be kept in mind, however, that $\mathbb{A}$ is defined for any value of the lattice spacing a, so it does not correspond to the continuum gauge field. According to (A6), the latter is obtained from $\mathbb{A}$ only in the continuum limit $a \to 0$.

We shall first recall the usual derivation in the case of the Landau gauge, corresponding to $\bar{A} = 0$, before considering the general case for which $\bar{A} \neq 0$. In this latter case, we shall consider both the formulation in terms of periodic links and the formulation in terms of twisted links.

1. Landau gauge

Consider a configuration $U_\mu(n)$ that extremizes the functional

$$F[U] \equiv \sum_{n,\mu} \mathrm{Re\,tr}\, U_\mu(n), \tag{A8}$$

along the corresponding $\mathcal{G}_0$-orbit. This means that for any $g_0 \approx \mathbb{1} + i\theta$, with $\theta^\dagger = \theta$, we should have

$$F[U^{\mathbb{1}+i\theta}] = F[U] + \mathcal{O}(\theta^2). \tag{A9}$$

Now, it is easily checked that

$$F[U^{\mathbb{1}+i\theta}] = F[U] - \sum_{n,\mu} \mathrm{Im\ tr}\,\theta(n)[U_\mu(n) - U_\mu(n-\hat{\mu})] + \mathcal{O}(\theta^2), \tag{A10}$$

from which we deduce that

$$\sum_{n,\mu} \mathrm{Im\ tr}\,\theta(n)[U_\mu(n) - U_\mu(n-\hat{\mu})] = 0. \tag{A11}$$

Given that this is true for any Hermitian matrix field $\theta(n) = \theta^a(n)t^a$, it follows that

$$\sum_{\mu} \mathrm{Im\ tr}\, t^a[U_\mu(n) - U_\mu(n-\hat{\mu})] = 0, \tag{A12}$$

which, owing to (A7) and after dividing by a^2, is rewritten as

$$\sum_{\mu} \frac{\mathbb{A}^a_\mu(n) - \mathbb{A}^a_\mu(n-\hat{\mu})}{a} = 0. \tag{A13}$$

The corresponding condition for the continuum gauge field is found upon using (A6). One obtains

$$\sum_{\mu} \frac{A^a_\mu(x) - A^a_\mu(x - a\hat{\mu})}{a} = \mathcal{O}(a^2), \tag{A14}$$

where the order $\mathcal{O}(a^2)$ comes from the fact that

$$\mathbb{A}^a_\mu(n) - \mathbb{A}^a_\mu(n-\hat{\mu}) = A^a_\mu(x) - A^a_\mu(x - a\hat{\mu}) + \mathcal{O}(a^3), \tag{A15}$$

because the two $\mathcal{O}(a^2)$ contributions that are subtracted from (A6) are located at points separated by one lattice spacing a. Equation (A14) then implies (summation over repeated indices implied)

$$\partial_\mu A^a_\mu(x) = 0, \tag{A16}$$

as expected.

2. Background Landau gauges

Let us now follow the same steps for the family of background gauges defined in (A1). We have this time

$$\tilde{F}[U^{\mathbb{1}+i\theta}] = \tilde{F}[U] - \sum_{n,\mu} \mathrm{Im\ tr}\,\theta(n)[U_\mu(n)e^{-ia\bar{A}\hat{\mu}_4} - e^{-ia\bar{A}\hat{\mu}_4}U_\mu(n-\hat{\mu})] + \mathcal{O}(\theta^2). \tag{A17}$$

It follows that the center-symmetric Landau gauge links obey the condition

$$\sum_\mu \mathrm{Im\ tr}\, t^a[U_\mu(n)e^{-ia\bar{A}\hat{\mu}_4} - e^{-ia\bar{A}\hat{\mu}_4}U_\mu(n-\hat{\mu})] = 0, \tag{A18}$$

which we rewrite for convenience as

$$\begin{aligned} 0 = &\sum_\mu \mathrm{Im\ tr}\, t^a[U_\mu(n), e^{-ia\bar{A}\hat{\mu}_4}] \\ &+ \sum_\mu \mathrm{Im\ tr}\, t^a[U_\mu(n) - U_\mu(n-\hat{\mu})] \\ &+ \sum_\mu \mathrm{Im\ tr}\, t^a(e^{-ia\bar{A}\hat{\mu}_4} - 1)[U_\mu(n) - U_\mu(n-\hat{\mu})]. \end{aligned} \tag{A19}$$

Note that this condition cannot be expressed solely in terms of $\mathbb{A}$, contrary to what happens in the Landau gauge. But we can always write

$$U_\mu(n) = \mathbb{C}_\mu(n)\mathbb{1} + (\mathbb{B}^a_\mu(n) + ia\mathbb{A}^a_\mu(n))t^a, \tag{A20}$$

$$e^{ia\bar{A}\hat{\mu}_4} = \bar{\mathbb{C}}(\hat{\mu})\mathbb{1} + (\bar{\mathbb{B}}^a(\hat{\mu}) + ia\bar{\mathbb{A}}^a(\hat{\mu}))t^a, \tag{A21}$$

with $\mathbb{A}^a_\mu(n)$ defined in Eq. (A7) and

$$\mathbb{B}^a_\mu(n) \equiv 2\mathrm{Re\ tr}[t^a U_\mu(n)]. \tag{A22}$$

Plugging these decompositions into the first two lines of Eq. (A19), we find

$$\begin{aligned} 0 = &\sum_\mu a[\mathbb{A}^a_\mu(n) - \mathbb{A}^a_\mu(n-\hat{\mu})] \\ &- \sum_\mu f^{abc}[a^2\bar{\mathbb{A}}^b(\hat{\mu})\mathbb{A}^c_\mu(n) + \bar{\mathbb{B}}^b(\hat{\mu})\mathbb{B}^c_\mu(n)] \\ &+ \sum_\mu \mathrm{Im\ tr}\, t^a(e^{-ia\bar{A}\hat{\mu}_4} - \mathbb{1})[U_\mu(n) - U_\mu(n-\hat{\mu})]. \end{aligned} \tag{A23}$$

The corresponding condition for the continuum gauge field is found upon using (A6) together with

$$\bar{\mathbb{A}}^a(\hat{\mu}) = \bar{A}^a_\mu + \mathcal{O}(a^2), \tag{A24}$$

$$\mathbb{B}^a_\mu(n) = \mathcal{O}(a^2), \tag{A25}$$

$$\bar{\mathbb{B}}^a(\hat{\mu}) = \mathcal{O}(a^2), \tag{A26}$$

$$U_\mu(n) - U_\mu(n-\hat{\mu}) = \mathcal{O}(a^2), \tag{A27}$$

with $\bar{A}^a_\mu = \delta_{\mu 4}\delta^{aj}\bar{A}^j$. After dividing by a^2, one obtains

$$\sum_\mu \left[\frac{A^a_\mu(x) - A^a_\mu(x-a\hat{\mu})}{a} - f^{abc}\bar{A}_\mu A^c_\mu(x)\right] = \mathcal{O}(a^2), \tag{A28}$$

which implies (summation over repeated indices implied)

$$\partial_\mu A^a_\mu(x) - f^{abc}\bar{A}^b_\mu A^c_\mu(x) = 0. \tag{A29}$$

Given that $\bar{A}_\mu$ is constant, this is rewritten as

$$\partial_\mu(A^a_\mu(x) - \bar{A}^a_\mu) - f^{abc}\bar{A}^b_\mu(A^c_\mu(x) - \bar{A}^c_\mu) = 0. \tag{A30}$$

We recognize here the background Landau gauge condition in the presence of the background $\bar{A}^a_\mu$. The particular choice (70) corresponding to $\bar{A}^3 = -(4\pi/3)T$ and $\bar{A}^8 = 0$ leads to the center-symmetric Landau gauge of Ref. [16], as announced.

3. Twisted links

Extending what we did in the main text, we can equivalently consider twisted links, defined from the periodic links as

$$\hat{U}_\mu(n) \equiv U^{g_{\bar{A}}}_\mu(n) \equiv g_{\bar{A}}(n)U_\mu(n)g^\dagger_{\bar{A}}(n+\hat{\mu}), \tag{A31}$$

with

$$g_{\bar{A}}(n) \equiv e^{ia\bar{A}n_4}. \tag{A32}$$

Since

$$e^{-ia\bar{A}\hat{\mu}_4} = g^\dagger_{\bar{A}}(n+\hat{\mu})g_{\bar{A}}(n), \tag{A33}$$

the functional $F_{\bar{A}}[U]$ defined in (A1) is rewritten as

$$\begin{aligned} F_{\bar{A}}[U] &= \sum_{n,\mu} \mathrm{Re\ tr}[g_{\bar{A}}(n)U_\mu(n)g^\dagger_{\bar{A}}(n+\hat{\mu})] \\ &= \sum_{n,\mu} \mathrm{Re\ tr}\hat{U}_\mu(n). \end{aligned} \tag{A34}$$

So, the twisted links are extrema of the Landau gauge functional (A8) but with different boundary conditions, as

they are nonperiodic. We deduce that they should obey the gauge-fixing condition

$$\sum_\mu \mathrm{Im\ tr} t^a[\hat{U}_\mu(n) - \hat{U}_\mu(n-\hat{\mu})] = 0. \tag{A35}$$

Alternatively, one can start from the gauge-fixing condition (A18) obeyed by the center-symmetric Landau gauge links. This condition is equivalent to the statement

$$\sum_\mu [U_\mu(n)e^{-ia\bar{A}\hat{\mu}_4} - e^{-ia\bar{A}\hat{\mu}_4}U_\mu(n-\hat{\mu})] = m_1\mathbb{1} + m_a t^a, \tag{A36}$$

for some $m_1 \in \mathbb{C}$ and $m_a \in \mathbb{R}$. Multiplying this equation on the left by $e^{ia\bar{A}\hat{\mu}_4}$ and on the right by $e^{-ia\bar{A}\hat{\mu}_4}$ while using Eq. (A31), we obtain

$$\sum_\mu [\hat{U}_\mu(n) - \hat{U}_\mu(n-\hat{\mu})] = m_1\mathbb{1} + \hat{m}_a t^a, \tag{A37}$$

for some new $\hat{m}_a \in \mathbb{R}$.[25] This latter condition is equivalent to (A35).

Proceeding as above, we introduce

$$\hat{\mathbb{A}}^a_\mu(n) \equiv 2\,\mathrm{Im\ tr}[t^a\hat{U}_\mu(n)] = \hat{A}^a_\mu(x) + \mathcal{O}(a^2), \tag{A38}$$

where $\hat{A}_\mu(x)$ denotes the "gauge field" associated with the twisted links. Then, Eq. (A35) is rewritten as

$$\sum_\mu \frac{\hat{\mathbb{A}}^a_\mu(n) - \hat{\mathbb{A}}^a_\mu(n-\hat{\mu})}{a} = 0 \tag{A39}$$

or

$$\sum_\mu \frac{\hat{A}^a_\mu(x) - \hat{A}^a_\mu(x-a\hat{\mu})}{a} = \mathcal{O}(a^2). \tag{A40}$$

This implies (summation over repeated indices implied)

$$\partial_\mu \hat{A}^a_\mu(x) = 0, \tag{A41}$$

which is the Landau gauge condition for $\hat{A}_\mu(x)$.

The gauge condition (A39) in terms of $\hat{\mathbb{A}}_\mu(n)$ looks way simpler than the gauge condition (A23) in terms of $\mathbb{A}_\mu(n)$, but this hides the fact that the relation between $\hat{\mathbb{A}}_\mu(n)$ and $\mathbb{A}_\mu(n)$ is a complicated one involving the $\mathbb{B}$'s, … as can be seen by taking the imaginary part of Eq. (A31) times t^a:

$$\hat{\mathbb{A}}^a_\mu(n) = \frac{2}{a}\mathrm{Im\ tr}[t^a g_{\bar{A}}(n)U_\mu(n)g^\dagger_{\bar{A}}(n+\hat{\mu})], \tag{A42}$$

which is not rewritten solely in terms of $\mathbb{A}^a_\mu(n)$.

[25] More precisely, one has $\hat{m}_a t^a = m_a g_c(n) t^a g^\dagger_c(n)$.

Yet, the relation between the associated continuum fields $\hat{A}_\mu(x)$ and $A_\mu(x)$ simplifies. To see this, we have to pay attention to the fact that $g_{\bar{A}}(n)$ cannot be expanded in a uniformly in n, since na is not small for $n_4 = L_4$. So, we first write

$$\begin{aligned}\hat{\mathbb{A}}^a_\mu(n) = &\frac{2}{a}\mathrm{Im\ tr}[t^a g_{\bar{A}}(n)U_\mu(n)g^\dagger_{\bar{A}}(n)] \\ &+\frac{2}{a}\mathrm{Im\ tr}[t^a g_{\bar{A}}(n)U_\mu(n)g^\dagger_{\bar{A}}(n)(e^{-ia\bar{A}\hat{\mu}_4}-1)],\end{aligned} \tag{A43}$$

and only expand the links and $e^{-ia\bar{A}\hat{\mu}_4} - 1$. This gives

$$\begin{aligned}\hat{\mathbb{A}}^a_\mu(n) = &(g_{\bar{A}}(n)A_\mu(x)g^\dagger_{\bar{A}}(n))^a \\ &- \bar{A}^a\delta_{\mu 4} + \mathcal{O}(a),\end{aligned} \tag{A44}$$

and so

$$\hat{A}^a_\mu(x) = (g_{\bar{A}}(x)A_\mu(x)g^\dagger_{\bar{A}}(x))^a - \bar{A}^a\delta_{\mu 4}, \tag{A45}$$

with $g_{\bar{A}}(x) = e^{i\bar{A}x_4}$. This also is rewritten as

$$\begin{aligned}\hat{A}^a_\mu(x) &= (g_{\bar{A}}(x)A_\mu(x)g^\dagger_{\bar{A}}(x))^a - ig_{\bar{A}}(x)\partial_\mu g^\dagger_{\bar{A}}(x) \\ &= (A^{g_{\bar{A}}}_\mu)^a(x).\end{aligned} \tag{A46}$$

So the continuum "gauge field" constructed from the twisted link acquires a simple interpretation as a nonperiodic gauge transformation of the gauge field associated with the periodic link.

In fact, it is precisely this relation that allows one to connect the continuum gauge conditions (A41) and (A30). This is because

$$\begin{aligned}\partial_\mu\hat{A}_\mu &= \partial_\mu\hat{A}_\mu + i[0_\mu, \hat{A}_\mu] \\ &= \partial_\mu A^{g_{\bar{A}}}_\mu + i[(0^{g^\dagger_{\bar{A}}}_\mu)^{g_{\bar{A}}}, A^{g_{\bar{A}}}_\mu] \\ &= g_{\bar{A}}(\partial_\mu A_\mu + i[0^{g^\dagger_{\bar{A}}}_\mu, A_\mu])g^\dagger_{\bar{A}}\end{aligned} \tag{A47}$$

and

$$0^{g^\dagger_{\bar{A}}}_\mu = -ig^\dagger_{\bar{A}}\partial_\mu g_{\bar{A}} = \bar{A}\delta_{\mu 4}. \tag{A48}$$

From this, it is easily seen that (A41) is equivalent to (A30).

APPENDIX B: WEYL BASES AND WEYL TRANSFORMATIONS

The calculations in the main text can be made more systematic upon introducing the defining and adjoint weights of SU(3) as well as Weyl bases and Weyl

transformations. This becomes particularly useful when dealing with higher link correlators, beyond the one-link average, and also when extending these considerations to SU(N) or other groups.

1. Weights, roots, and Weyl bases

A Weyl basis of the algebra is made of a maximal set [two in the case of SU(3)] of commuting generators denoted t^j and other generators denoted t^α that diagonalize simultaneously the adjoint action of all the t^j:

$$[t^j, t^\alpha] = \alpha^j t^\alpha. \tag{B1}$$

The labels α are [two-dimensional for SU(3)] real-valued vectors, known as roots, whose coordinates α^j correspond to the eigenvalues of the action of t^j in the adjoint representation. One can also diagonalize the action of the t^j in the defining (or fundamental) representation. In the vector space of the defining representation, this defines some vectors, denoted as kets $|\rho\rangle$ such that

$$t^j|\rho\rangle = \rho^j|\rho\rangle. \tag{B2}$$

The labels ρ are [two-dimensional for SU(3)] real-valued vectors, known as defining (or fundamental) weights, whose coordinates ρ^j correspond to the eignevalues of the action of t^j in the defining representation. For SU(3), there are three defining weights

$$\begin{aligned}\rho_1 &= \left(\frac{1}{2}, \frac{1}{2\sqrt{3}}\right),\\ \rho_2 &= \left(-\frac{1}{2}, \frac{1}{2\sqrt{3}}\right),\\ \rho_3 &= \left(0, -\frac{1}{\sqrt{3}}\right),\end{aligned} \tag{B3}$$

and six roots obtained as all possible, nonvanishing differences of defining weights, $\alpha_{ij} \equiv \rho_i - \rho_j$, with $i \neq j$.

The links can be decomposed along two appropriate bases:

$$\begin{aligned}U_\mu(n) &= \sum_{\rho'\rho} U_\mu^{\rho'\rho}(n)|\rho'\rangle\langle\rho|\\ &= U_\mu^1(n)\mathbb{1} + \sum_j U_\mu^j(n)t^j + \sum_\alpha U_\mu^\alpha(n)t^\alpha.\end{aligned} \tag{B4}$$

We note that, if the t^j are chosen diagonal, the $|\rho\rangle$ simply correspond to the canonical basis, made of vectors with only one nonzero entry, equal to 1, the basis which we have considered in the main text. But the notation in terms of the weights ρ is more useful since it allows for a geometrical interpretation. The relation between the two bases is easily found. In particular,[26]

$$U_\mu^1(n) = \frac{1}{N}\sum_\rho U_\mu^{\rho\rho}(n), \tag{B5}$$

$$U_\mu^j(n) = 2\sum_\rho \rho^j U_\mu^{\rho\rho}(n). \tag{B6}$$

2. Weyl transformations

With each root α, one can associate a particular color rotation, known as a Weyl transformation W_α (see for instance [17]). Here, we will need to know only that

$$W_\alpha(X\cdot t)W_\alpha^\dagger = (R_\alpha X)\cdot t, \tag{B7}$$

where R_α is the reflection with respect to an axis orthogonal to the root α, and we have introduced the shorthand notation $X\cdot t \equiv X^j t^j$. Moreover,

$$W_\alpha|\rho\rangle = |R_\alpha\rho\rangle. \tag{B8}$$

With these definitions and properties at hand, a possible candidate for $\tilde{g}(n)$ obeying Eq. (61) is

$$\tilde{g}(n) = W_{\alpha_{13}}W_{\alpha_{12}}e^{-i\frac{n_4}{L_4}4\pi\rho_1\cdot t}. \tag{B9}$$

This form is reminiscent from the one found in Ref. [17]. Using Eq. (B7), one finds

$$\begin{aligned}&\tilde{g}(n)e^{-i\frac{4\pi\hat{\mu}_4\lambda_3}{3L_4{}^2}}\tilde{g}^\dagger(n+\hat{\mu})\\ &= W_{\alpha_{13}}W_{\alpha_{12}}e^{-i\frac{n_4}{L_4}4\pi\rho_1^j t^j}e^{-i\frac{4\pi\hat{\mu}_4\lambda_3}{3L_4{}^2}}e^{i\frac{n_4+\hat{\mu}_4}{L_4}4\pi\rho_1^j t^j}W_{\alpha_{12}}^\dagger W_{\alpha_{13}}^\dagger\\ &= W_{\alpha_{13}}W_{\alpha_{12}}e^{-i\frac{\hat{\mu}_4}{L_4}(r_c-4\pi\rho_1)\cdot t}W_{\alpha_{12}}^\dagger W_{\alpha_{13}}^\dagger\\ &= e^{-i\frac{\hat{\mu}_4}{L_4}(R_{\alpha_{13}}R_{\alpha_{12}}(r_c-4\pi\rho_1))\cdot t},\end{aligned} \tag{B10}$$

where $r_c = (4\pi/3, 0)$. Now, it is easily checked that $R_{\alpha_{13}}R_{\alpha_{12}}$ is nothing but the rotation $\mathcal{R}$ by an angle $2\pi/3$ and that $\mathcal{R}(r_c - 4\pi\rho_1) = r_c$. Thus, as announced we have recovered Eq. (B9).

We can now have a look at how a general diagonal matrix

$$X = \sum_\rho X^{\rho\rho}|\rho\rangle\langle\rho|, \tag{B11}$$

expressed in the Cartan-Weyl basis, transforms under $\tilde{g}$. We first write

[26]Moreover, one can arrange the bases such that $U_\mu^\alpha = U_\mu^{\rho\rho'}$, with $\alpha = \rho - \rho'$.

$$\begin{aligned}\tilde{g}(n)|\rho\rangle &= W_{\alpha_{13}} W_{\alpha_{12}} e^{-i\frac{n_4}{L_4}4\pi\rho_1\cdot t}|\rho\rangle \\ &= e^{-i\frac{n_4}{L_4}4\pi\rho_1\cdot\rho} W_{\alpha_{13}} W_{\alpha_{12}}|\rho\rangle \\ &= e^{-i\frac{n_4}{L_4}4\pi\rho_1\cdot\rho}|R_{\alpha_{13}} R_{\alpha_{12}}\rho\rangle \\ &= e^{-i\frac{n_4}{L_4}4\pi\rho_1\cdot\rho}|\mathcal{R}\rho\rangle, \end{aligned} \tag{B12}$$

where we used Eqs. (B2) and (B8). Then,

$$\begin{aligned}\tilde{g}(n) X g(n+\hat{\mu}) &= \sum_\rho X^{\rho\rho}\tilde{g}(n)|\rho\rangle\langle\rho|\tilde{g}^\dagger(n+\hat{\mu}) \\ &= \sum_\rho X^{\rho\rho} e^{i\frac{\hat{\rho}_4}{L_4}4\pi\rho_1\cdot\rho}|\mathcal{R}\rho\rangle\langle\mathcal{R}\rho| \\ &= \sum_\rho X^{\mathcal{R}^{-1}\rho\mathcal{R}^{-1}\rho} e^{i\frac{\hat{\rho}_4}{L_4}4\pi\rho_1\cdot(\mathcal{R}^{-1}\rho)}|\rho\rangle\langle\rho|. \end{aligned} \tag{B13}$$

Using the explicit values for the ρ's given above [see Eq. (B3)], we retrieve the transformation (63).

In the case of the twisted links, the relevant transformation is

$$\begin{aligned}\hat{g}(n) &\equiv g_c(n)\tilde{g}(n)g_c^\dagger(n) \\ &= e^{-i\frac{n_4}{L_4}\frac{4\pi}{3}\frac{\lambda_3}{2}} W_{\alpha_{13}} W_{\alpha_{12}} e^{-i\frac{n_4}{L_4}4\pi\rho_1^j t^j} e^{i\frac{n_4}{L_4}\frac{4\pi}{3}\frac{\lambda_3}{2}}, \end{aligned} \tag{B14}$$

which acts on the link as a local color rotation (see the main text for details). Because of that, the n_4-dependent factors do not play any role when $\hat{g}$ acts on a diagonal matrix. We are thus led to consider

$$\begin{aligned}\hat{g}(n) X \hat{g}^\dagger(n) &= W_{\alpha_{13}} W_{\alpha_{12}} X W_{\alpha_{12}}^\dagger W_{\alpha_{13}}^\dagger \\ &= \sum_\rho X^{\rho\rho} W_{\alpha_{13}} W_{\alpha_{12}}|\rho\rangle\langle\rho| W_{\alpha_{12}}^\dagger W_{\alpha_{13}}^\dagger \\ &= \sum_\rho X^{\rho\rho}|\mathcal{R}\rho\rangle\langle\mathcal{R}\rho| \\ &= \sum_\rho X^{\mathcal{R}^{-1}\rho\mathcal{R}^{-1}\rho}|\rho\rangle\langle\rho|, \end{aligned} \tag{B15}$$

where we have used Eq. (B8). This leads to the transformation

$$X^{\rho\rho} \to X^{\mathcal{R}^{-1}\rho\mathcal{R}^{-1}\rho}. \tag{B16}$$

Using the explicit values for the ρ's given above, we retrieve the cyclic permutation (110).

An even more convenient way to proceed is to express this transformation in the second basis in (B4). Using Eq. (B5), we find that

$$\begin{aligned} X^j &\to \sum_\rho \rho^j X^{\mathcal{R}^{-1}\rho\mathcal{R}^{-1}\rho} \\ &= \sum_\rho (\mathcal{R}\rho)^j X^{\rho\rho} \\ &= \mathcal{R}_k^j \sum_\rho \rho^k X^{\rho\rho} = \mathcal{R}_k^j X^k, \end{aligned} \tag{B17}$$

which is the rotation by an angle $2\pi/3$ referred to below Eq. (119). This result could have also been obtained by working directly in the second basis. Indeed,

$$\begin{aligned}&\hat{g}(n)\left(X_1\mathbb{1} + \sum_j X^j t^j\right)\hat{g}^\dagger(n) \\ &= X_1\mathbb{1} + \sum_j \hat{g}(n) X^j t^j \hat{g}^\dagger(n) \\ &= X_1\mathbb{1} + \sum_j W_{\alpha_{13}} W_{\alpha_{12}} X^j t^j W_{\alpha_{12}}^\dagger W_{\alpha_{13}}^\dagger \\ &= X_1\mathbb{1} + \sum_j (\mathcal{R}X)^j t^j, \end{aligned} \tag{B18}$$

where we have used Eq. (B7).

APPENDIX C: LINK AVERAGES

The more precise form of the link averages in Sec. V E are

$$\langle U_4\rangle = \begin{pmatrix} 0.8687(92) - 0.123(26)i & 0.023(27) + 0.014(19)i & 0.020(18) - 0.049(19)i \\ -0.001(27) + 0.015(20)i & 0.8662(99) + 0.131(26)i & -0.001(20) + 0.004(21)i \\ -0.027(18) - 0.040(20)i & -0.002(22) + 0.006(20)i & 0.8853(86) - 0.009(24)i \end{pmatrix}, \tag{C1}$$

$$\langle U_4^{\tilde{g}}\rangle = \begin{pmatrix} 0.829(12) - 0.312(21)i & 0.005(18) - 0.048(21)i & 0.006(21) - 0.000(23)i \\ 0.002(18) - 0.0522(21)i & 0.744(16) + 0.464(21)i & 0.005(21) - 0.026(25)i \\ -0.004(25) + 0.000(19)i & -0.0110(25) - 0.011(22)i & 0.8588(86) - 0.173(23)i \end{pmatrix}, \tag{C2}$$

$$\langle U_4^{\tilde{g}^\dagger}\rangle = \begin{pmatrix} 0.748(14) - 0.457(22)i & -0.003(21)7 - 0.002(21)i & -0.00(25) + 0.014(24)i \\ 0.006(19) - 0.002(26)i & 0.8352(97) + 0.294(24)i & -0.047(19) + 0.012(18)i \\ 0.026(25) - 0.004(22)i & 0.039(18) + 0.035(20)i & 0.858(11) + 0.182(25)i \end{pmatrix}, \tag{C3}$$

for the ensemble averages of the temporal link at the origin of the high temperature $64^3 \times 6$ lattice, and

$$\langle U_4 \rangle = \begin{pmatrix} 0.829(10) - 0.194(25)i & -0.021(21) + 0.054(24)i & -0.022(24) + 0.013(26)i \\ 0.006(23) + 0.045(24)i & 0.827(11) + 0.241(28)i & 0.003(24) - 0.022(19)i \\ 0.024(24) + 0.024(24)i & 0.018(24) - 0.020(21)i & 0.8476(95) - 0.050(27)i \end{pmatrix}, \tag{C4}$$

$$\langle U_4^{\tilde{g}} \rangle = \begin{pmatrix} 0.806(12) - 0.267(28)i & 0.009(23)7 + 0.033(22)i & -0.024(21) - 0.012(26)i \\ -0.017(24) + 0.018(24)i & 0.815(11) + 0.247(25)i & 0.058(22) + 0.006(24)i \\ 0.02(21)2 - 0.003(25)i & -0.042(22) - 0.017(25)i & 0.8611(99) + 0.019(26)i \end{pmatrix}, \tag{C5}$$

$$\langle U_4^{\tilde{g}^\dagger} \rangle = \begin{pmatrix} 0.837(13) - 0.204(26)5i & 0.020(21)2 + 0.009(24)i & -0.006(25) + 0.045(23)i \\ -0.026(20) - 0.006(27)i & 0.832(11) + 0.171(27)i & 0.029(25) - 0.017(22)i \\ 0.009(24) + 0.057(22)i & -0.007(27) - 0.024(23)i & 0.8506(97) + 0.027(26)i \end{pmatrix}, \tag{C6}$$

for the ensemble averages of the temporal link at the origin of the low temperature $64^3 \times 8$ lattice.

As for the combined ensemble and lattice averages, we find

$$\langle\langle U_4 \rangle\rangle = \begin{pmatrix} 0.853201(34) - 0.14567(16)i & -0.0000002(71) + 0.0000078(69)i & -0.0000038(70) - 0.0000023(72)i \\ -0.0000002(71) - 0.0000078(69)i & 0.853206(40) + 0.14559(18)i & -0.0000094(81) - 0.0000087(70)i \\ -0.0000028(68) + 0.0000035(72)i & -0.0000118(80) + 0.0000050(72)i & 0.866012(17) + 0.00009(15)i \end{pmatrix}, \tag{C7}$$

$$\langle\langle U_4^{\tilde{g}} \rangle\rangle = \begin{pmatrix} 0.813815(56) - 0.29611(14)i & 0.0000140(56) - 0.0000043(65)i & 0.0000087(72) + 0.0000094(83)i \\ 0.0000149(56) + 0.0000043(65)i & 0.747226(90) + 0.43683(16)i & 0.0000056(61) - 0.0000015(76)i \\ 0.0000050(75) - 0.0000118(82)i & 0.0000048(59) + 0.0000034(75)i & 0.851544(32) - 0.15501(17)i \end{pmatrix}, \tag{C8}$$

$$\langle\langle U_4^{\tilde{g}^\dagger} \rangle\rangle = \begin{pmatrix} 0.747174(82) - 0.43691(15)i & -0.0000050(66) - 0.0000038(59)i & 0.0000015(75) - 0.0000056(65)i \\ -0.0000050(66) + 0.0000038(59)i & 0.813756(52)1 + 0.29627(13)i & 0.0000023(75) + 0.0000038(73)i \\ 0.0000033(74) + 0.0000048(62)i & 0.0000035(71) - 0.0000028(73)i & 0.851569(32) + 0.15492(16)i \end{pmatrix}, \tag{C9}$$

over the high temperature $64^3 \times 6$ lattice, and

$$\langle\langle U_4 \rangle\rangle = \begin{pmatrix} 0.83362(15) - 0.21910(51)i & -0.0000013(84) - 0.0000034(86)i & -0.000001(10) + 0.0000084(94)i \\ -0.0000013(84) + 0.0000034(86)i & 0.83352(12) + 0.21939(45)i & -0.0000008(85) - 0.0000084(82)i \\ -0.000003(10) - 0.0000079(88)i & -0.0000029(81) + 0.0000079(83)i & 0.861665(24) - 0.00031(50)i \end{pmatrix}, \tag{C10}$$

$$\langle\langle U_4^{\tilde{g}} \rangle\rangle = \begin{pmatrix} 0.83222(14) - 0.22331(53)i & 0.0000109(81) + 0.0000101(86)i & 0.0000084(85) + 0.0000008(86)i \\ 0.0000109(81) - 0.0000101(86)i & 0.83149(14) + 0.22706(52)i & -0.0000024(78) - 0.0000097(90)i \\ 0.0000079(84) - 0.0000029(80)i & -0.0000048(82) + 0.0000087(85)i & 0.861905(26) - 0.00382(46)i \end{pmatrix}, \tag{C11}$$

$$\langle\langle U_4^{\tilde{g}^\dagger}\rangle\rangle = \begin{pmatrix} 0.83155(12) - 0.22676(42)i & 0.0000010(88) - 0.0000072(86)i & 0.0000097(91) + 0.0000024(79)i \\ 0.0000010(88)0.0000072(86)i & 0.83238(14) + 0.22272(51)i & -0.0000084(90) + 0.0000009(93)i \\ 0.0000087(88) - 0.0000048(83)i & -0.0000079(89) - 0.0000031(95)i & 0.861921(23) + 0.00412(49)i \end{pmatrix}, \tag{C12}$$

over the low temperature $64^3 \times 8$ lattice.

APPENDIX D: BASIC STEEPEST ASCENT ALGORITHM

Let us here show that the basic steepest ascent algorithm applied to a center-symmetric gauge functional $\tilde{F}[U]$ is symmetry preserving in the sense that, starting from two configurations U and $U^{\tilde{g}}$ related by the transformation $\tilde{g}$ that leaves the functional $\tilde{F}[U]$ invariant, the two maxima U^{g_0} and $(U^{\tilde{g}})^{g_0'}$ that are selected by the steepest ascent algorithm, along the $\mathcal{G}_0$-orbits of U and $U^{\tilde{g}}$, are also related by $\tilde{g}$:

$$(U^{\tilde{g}})^{g_0'} = (U^{g_0})^{\tilde{g}}. \tag{D1}$$

Let us first explain how a local maximum is found starting from $U_\mu(n)$. One first constructs the gradient

$$X^a[U](n) \equiv \left.\frac{\delta \tilde{F}[U^{e^{i\theta^b t^b}}]}{\delta\theta^a(n)}\right|_{\theta=0}, \tag{D2}$$

and builds an ascent gauge transformation

$$g_0[U;\lambda] = \exp\{i\lambda X^a[U]t^a\}, \tag{D3}$$

with λ some adjustable parameter, taking for instance the trial values $1 \to 1/2 \to 1/4 \to \cdots$ until $\tilde{F}[U^{g_0[U;\lambda]}]$ exceeds $\tilde{F}[U]$. After one step, the procedure produces one value of λ denoted λ_1 as well as $U_1 \equiv U^{g_0[U;\lambda_1]}$ which can be used as a new link to continue the ascent. Repeating the procedure many times, one obtains a collection of numbers λ_i as well as intermediate links $U_i \equiv U^{g_0[U_{i-1};\lambda_i]}$ which are closer and closer to a maximum. The procedure stops whenever the gradient becomes compatible with zero in which case one has reached a maximum.[27]

The question is now: what happens if we start from $U_\mu^{\tilde{g}}$ instead? How are the corresponding λ_i's and intermediate links related to the previous ones? To answer this question, we use Eq. (50) to write

$$\begin{aligned}\tilde{F}[(U^{\tilde{g}})^{g_0}] &= \tilde{F}[U^{g_0\tilde{g}}] \\ &= \tilde{F}[(U^{\tilde{g}^\dagger g_0 \tilde{g}})^{\tilde{g}}] \\ &= \tilde{F}[U^{\tilde{g}^\dagger g_0 \tilde{g}}].\end{aligned} \tag{D4}$$

From this, we can deduce a relation between the gradients at U and $U^{\tilde{g}}$, namely (pay attention to the ordering of $\tilde{g}$, t^a, and $\tilde{g}^\dagger$ when performing the chain rule)

$$X^a[U^{\tilde{g}}](n)t^a = X^a[U](n)\tilde{g}(n)t^a\tilde{g}^\dagger(n), \tag{D5}$$

from which it follows that

$$g_0[U^{\tilde{g}};\lambda] = \tilde{g}g_0[U,\lambda]\tilde{g}^\dagger, \tag{D6}$$

and thus,

$$\begin{aligned}(U^{\tilde{g}})^{g_0[U^{\tilde{g}};\lambda]} &= (U^{\tilde{g}})^{\tilde{g}g_0[U,\lambda]\tilde{g}^\dagger} \\ &= U^{\tilde{g}g_0[U,\lambda]} \\ &= (U^{g_0[U,\lambda]})^{\tilde{g}}.\end{aligned} \tag{D7}$$

Then,

$$\tilde{F}[(U^{\tilde{g}})^{g_0[U^{\tilde{g}};\lambda]}] = \tilde{F}[U^{g_0[U;\lambda]}]. \tag{D8}$$

This means the adjustment λ_1 is the same as before (if one uses the same algorithm $1 \to 1/2 \to 1/4 \to \cdots$). And moreover,

$$V_1 \equiv (U^{\tilde{g}})^{g_0[U^{\tilde{g}};\lambda_1]} = (U^{g_0[U,\lambda_1]})^{\tilde{g}} = U_1^{\tilde{g}}. \tag{D9}$$

From this we deduce that, along the ascent from U or $U^{\tilde{g}}$, all λ_i's are the same and the intermediate links are related as $V_i = U_i^{\tilde{g}}$. This ensures that the final, extremal configurations are also related by $\tilde{g}$ which ensures that $\mathcal{E}_{\rm gf}^{\tilde{g}} \simeq \mathcal{E}_{\rm gf}$ in the symmetric phase.

We have implemented the simple steepest ascent algorithm described in Sec. IV E for the functional (70) on a one-dimensional lattice of L sites. In Fig. 7, we show, in the complex plane, the three diagonal components of the links, elevated to the power L for convenience, along the ascent to the maximum of $\tilde{F}[U]$. We start from two different link configurations related by the transformation $\tilde{g}$ in Eq. (62). The diagonal components of these initial configurations are related by (63)–(66). By elevating the components to the

[27] In fact, it could happen that one reaches more generally an extremum. But looking for maxima is just a numerical convenience and, if one ends up with some extrema, there is no problem in including them in the definition of the gauge-fixed configurations.

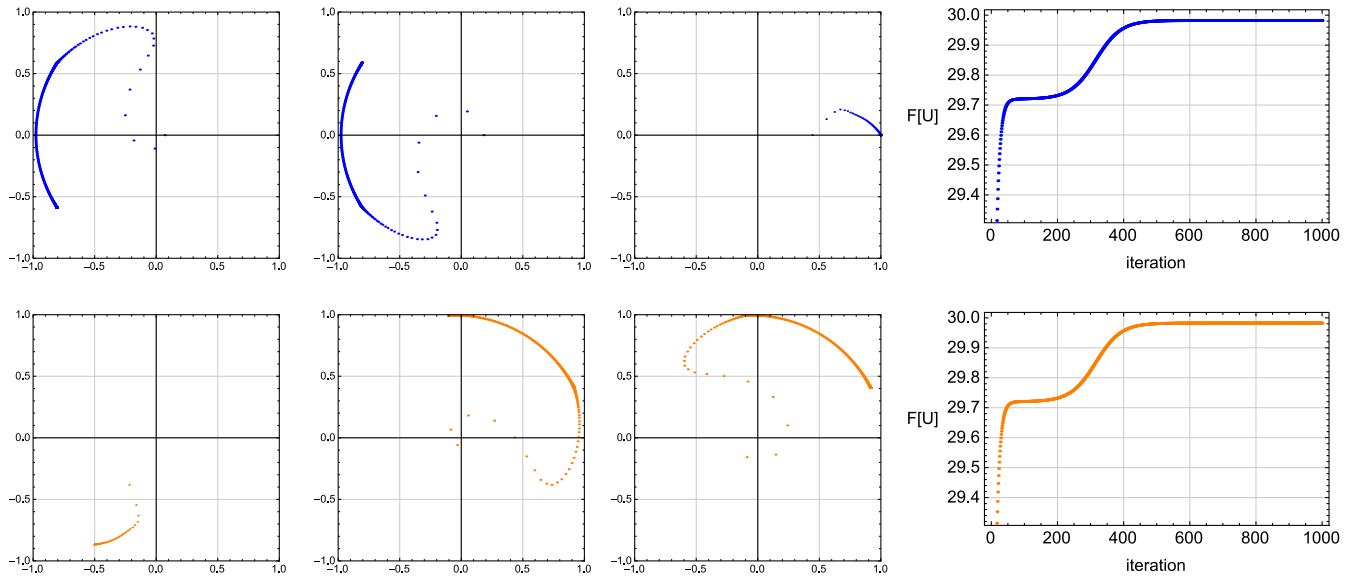


FIG. 7. The three diagonal components (from left to right but one) of the link elevated to the power L (number of lattice sites) at a given site of a $1d$ lattice along the ascent to the maximum of $\tilde{F}[U]$. The top and bottom plots differ by the starting links which are chosen to be related by the center transformations $\tilde{g}$. The right-most plot shows the value of $\tilde{F}[U]$ along the ascent. This function is exactly the same for the two ascents considered here.

power L, the relations involve simple phases $e^{\pm i2\pi/3}$ which one can easily identify in the plots. What the plots show is that these relations are preserved along the ascent to the maximum, thus confirming that this simple implementation of the steepest ascent algorithm preserves the $\tilde{g}$-invariance of the ensemble.

[1] R. D. Pisarski, arXiv:hep-ph/0203271.
[2] J. Greensite, *An Introduction to the Confinement Problem*, Lecture Notes in Physics (Springer Berlin, Heidelberg, 2011).
[3] R. V. Gavai, Nucl. Phys. **B215**, 458 (1983).
[4] R. V. Gavai and F. Karsch, Phys. Lett. **125B**, 406 (1983).
[5] T. Celik, J. Engels, and H. Satz, Phys. Lett. **125B**, 411 (1983).
[6] B. Svetitsky, Phys. Rep. **132**, 1 (1986).
[7] D. M. van Egmond and U. Reinosa, Phys. Rev. D **108**, 054029 (2023).
[8] A. M. Polyakov, Phys. Lett. **72B**, 477 (1978).
[9] T. K. Herbst, J. Luecker, and J. M. Pawlowski, arXiv:1510.03830.
[10] J. Braun, H. Gies, and J. M. Pawlowski, Phys. Lett. B **684**, 262 (2010).
[11] J. Braun, A. Eichhorn, H. Gies, and J. M. Pawlowski, Eur. Phys. J. C **70**, 689 (2010).
[12] L. F. Abbott, Nucl. Phys. **B185**, 189 (1981).
[13] L. F. Abbott, Acta Phys. Pol. B **13**, 33 (1982).
[14] L. Fister and J. M. Pawlowski, Phys. Rev. D **88**, 045010 (2013).
[15] U. Reinosa, Lect. Notes Phys. **1006** (2022).
[16] D. M. van Egmond, U. Reinosa, J. Serreau, and M. Tissier, SciPost Phys. **12**, 087 (2022).
[17] D. M. van Egmond and U. Reinosa, Phys. Rev. D **109**, 036002 (2024).
[18] D. M. van Egmond and U. Reinosa, Phys. Rev. D **106**, 074005 (2022).
[19] G. Curci and R. Ferrari, Nuovo Cimento A **32**, 151 (1976).
[20] M. Peláez, U. Reinosa, J. Serreau, M. Tissier, and N. Wschebor, Rep. Prog. Phys. **84**, 124202 (2021).
[21] A. Cucchieri and T. Mendes, Proc. Sci. FACESQCD2010 (**2010**) 007.
[22] C. S. Fischer, A. Maas, and J. A. Muller, Eur. Phys. J. C **68**, 165 (2010).
[23] A. Maas, J. M. Pawlowski, L. von Smekal, and D. Spielmann, Phys. Rev. D **85**, 034037 (2012).
[24] T. Mendes and A. Cucchieri, Proc. Sci. LATTICE2014 (**2015**) 183.
[25] P. J. Silva, O. Oliveira, P. Bicudo, and N. Cardoso, Phys. Rev. D **89**, 074503 (2014).
[26] R. Aouane, V. G. Bornyakov, E. M. Ilgenfritz, V. K. Mitrjushkin, M. Muller-Preussker, and A. Sternbeck, Phys. Rev. D **85**, 034501 (2012).
[27] L. Fister and J. M. Pawlowski, arXiv:1112.5440.

[28] M. Quandt and H. Reinhardt, Phys. Rev. D **92**, 025051 (2015).
[29] P. J. Silva and O. Oliveira, Phys. Rev. D **93**, 114509 (2016).
[30] C. Gattringer, Phys. Lett. B **690**, 179 (2010).
[31] R. G. Edwards, and B. Joó, Nucl. Phys. B, Proc. Suppl. **140**, 832 (2005).
[32] M. Pippig, SIAM J. Sci. Comput. **35**, C213 (2013).
[33] O. Oliveira and P. J. Silva, Phys. Rev. D **86**, 114513 (2012).
[34] M. A. Shifman, A. I. Vainshtein, and V. I. Zakharov, Nucl. Phys. B **147**, 385 (1979).
[35] G. Martinelli and C. T. Sachrajda, Nucl. Phys. **B478**, 660 (1996).
[36] R. Horsley, G. Hotzel, E. M. Ilgenfritz, R. Millo, H. Perlt, P. E. L. Rakow, Y. Nakamura, G. Schierholz, and A. Schiller, Phys. Rev. D **86**, 054502 (2012).
[37] 10.54499/UIDB/04564/2020.
[38] 10.54499/UIDP/04564/2020.
[39] 10.54499/CERN/FIS-PAR/0023/2021.
[40] 10.54499/CEECIND/00488/2017/CP1460/CT0030.
[41] http://www.uc.pt/lca.
[42] http://macc.fccn.pt.
[43] 10.54499/2021.09759.CPCA.